

000 001 002 003 004 005 006 007 008 009 010 011 012 013 014 015 016 017 018 019 020 021 022 023 024 025 026 027 028 029 030 031 032 033 034 035 036 037 038 039 040 041 042 043 044 045 046 047 048 049 050 051 052 053 LEARNING ON THE JOB: TEST-TIME CURRICULA FOR TARGETED REINFORCEMENT LEARNING

Anonymous authors

Paper under double-blind review

ABSTRACT

Humans are good at learning on the job: We learn how to solve the tasks we face as we go along. Can a model do the same? We propose an agent that assembles a task-specific curriculum, called *test-time curriculum* (TTC-RL), and applies reinforcement learning to continue training the model for its target task. The test-time curriculum avoids time-consuming human curation of datasets by automatically selecting the most task-relevant data from a large pool of available training data. Our experiments demonstrate that reinforcement learning on a test-time curriculum consistently improves the model on its target tasks, across a variety of evaluations and models. Notably, on challenging math and coding benchmarks, TTC-RL improves the pass@1 of Qwen3-8B by approximately 1.8x on AIME25 and 2.1x on CodeElo. Moreover, we find that TTC-RL significantly raises the performance ceiling compared to the initial model, increasing pass@8 on AIME25 from 40% to 62% and on CodeElo from 28% to 43%. Our findings show the potential of test-time curricula in extending the test-time scaling paradigm to continual training on thousands of task-relevant experiences during test-time.

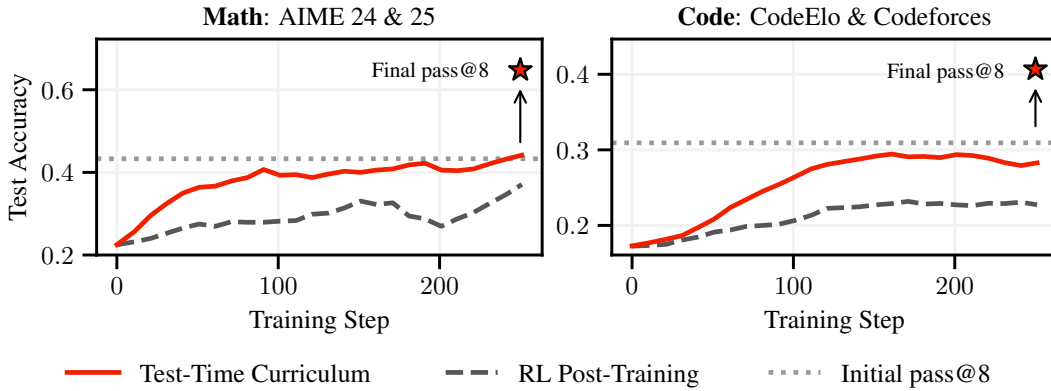


Figure 1: **Test-time curricula (TTCs) lead to remarkable improvements in math and coding by practicing on self-curated task-related problems at test-time.** The plots show the pass@1 test accuracy of Qwen3-8B throughout its test-time training. Our method, TTC-RL (solid red line), consistently improves performance, learning faster and achieving a higher final accuracy than standard RL post-training (dashed gray line). Notably, the final pass@1 accuracy of TTC-RL approaches the model’s initial pass@8 performance (dotted gray line), which represents a proxy for the performance ceiling of the initial model. The stars indicate the final pass@8 values after TTC-RL, demonstrating a significant improvement over the initial pass@8, which indicates that the model learns new solution strategies at test-time.

1 INTRODUCTION

We study how large language models (LLMs) can continually improve at reasoning on their target tasks at test-time. Increasing test-time compute, for example, by extended use of context as scratch space, has recently emerged as a key direction for improving LLMs on challenging tasks such as math and coding (Jaech et al., 2024; Guo et al., 2025; Kimi et al., 2025). Test-time scaling has been

054 driven primarily by extensive general-purpose reinforcement learning (RL; [Guo et al., 2025](#)), where
 055 the LLM learns how to effectively use its context for reasoning. However, since the context of
 056 LLMs is bounded and becomes exceedingly expensive to expand, an LLM cannot learn in-context
 057 from experience over long timeframes.

058 One promising technique for overcoming this challenge is test-time training (TTT; [Sun et al., 2020](#);
 059 [Hardt & Sun, 2024](#)), which continues training the model at test-time after being given a task.
 060 Previous work has studied TTT via supervised fine-tuning on human-created or expert data, either
 061 retrieved ([Hardt & Sun, 2024](#); [Hübotter et al., 2025](#)) or provided as few-shot examples ([Akyürek et al., 2025](#)).
 062 Other work has instead focused on TTT in the context of recurrent neural networks ([Sun et al., 2025](#);
 063 [von Oswald et al., 2025](#); [Zhang et al., 2025b](#)), aiming to replace the costly
 064 attention-based context in Transformers ([Vaswani et al., 2017](#)) with a fixed-size state (i.e., the model
 065 itself), but losing some of the advantages of reasoning over an uncompressed scratchpad. We explore
 066 a complementary approach to test-time scaling, where an LLM is continually *trained* on self-curated
 067 training tasks related to its target task, while practicing on each individual training task in-context.
 068 This leverages the Transformer’s attention as an uncompressed scratchpad for short-term ideation,
 069 while meta-learning strategies for leveraging that context across long-term, task-specific experience.

070 We propose a *test-time curriculum* (TTC) agent that automatically designs its own curriculum of
 071 training tasks by selecting the relevant tasks for the job from a large corpus of existing tasks. The
 072 agent then attempts tasks in its curriculum, and compresses the gathered experience into its weights
 073 via RL. The automatic self-guided curriculum design avoids laborious human curation of datasets,
 074 and enables training on purpose-built curricula at test-time. We find that this *reinforcement learning on*
 075 *test-time curricula* (TTC-RL) leads to remarkably improved reasoning on target tasks. In
 076 particular, we find that TTC-RL improves the pass@1 of several strong LLMs across diverse
 077 reasoning tasks, covering competition math, coding, and scientific reasoning (cf. Figure 1). We further
 078 identify that TTC-RL is complementary to other means of test-time scaling, effectively improving
 079 pass@ k and maj@ k even at large k . Notably, we find that TTC-RL can overcome the limitation of
 080 fixed context windows by observing that a non-thinking model (limited to 8k context tokens) with
 081 TTC-RL can perform similarly to the same model thinking for 30k tokens in-context. This demon-
 082 strates that during TTC-RL, the model continues *learning* how to think effectively for its target tasks.
 083 Our results suggest such targeted RL as a promising new direction for LLM agents that continually
 084 improve at test-time through many interactions with an environment.

084 We summarize our contributions as follows:

- 086 **1. We propose a TTC agent for targeted RL (§3):** We propose a test-time curriculum agent
 087 which at test-time when given a target task, self-selects related training tasks from a diverse
 088 corpus. The agent then learns from its own experience of attempting those tasks via RL.
- 089 **2. TTC-RL improves reasoning on target tasks (§4):** Across several models and tasks, TTC-
 090 RL consistently improves pass@1 substantially faster than general-purpose RL post-training
 091 on standard RL datasets, and saturates at a higher accuracy. Next, we identify that TTC-RL
 092 substantially raises the performance ceiling of the model (pass@ k) and demonstrate that it
 093 is complementary to existing approaches to test-time scaling. Finally, we find that TTC-RL
 094 yields strongly specialized models that perform remarkably well on their target tasks, even
 095 when compared to models that are allowed to think for tens of thousands of tokens in context.
- 096 **3. Measuring latent improvements in reasoning (§5):** The evaluation of RL-trained
 097 models faces the challenge of estimating whether improved scores are due to better reasoning or
 098 merely learning the expected output format. We introduce a new metric, *latent improvement*,
 099 which computes a lower bound on the improvement in reasoning due to RL training, and find
 100 that TTC-RL leads to substantial improvements in “latent” reasoning.

101 2 RELATED WORK

103 **Test-time scaling and general-purpose RL training.** A common strategy for improving LLM
 104 performance in challenging domains is to allocate additional test-time compute, for instance,
 105 through majority voting ([Snell et al., 2025](#)), search with a reward model ([Lightman et al., 2023](#);
 106 [Wang et al., 2024a](#); [Setlur et al., 2025a](#)), or by identifying consistent patterns among parallel
 107 rollouts ([Wang et al., 2023](#); [Huang et al., 2025a](#)). The potential of such methods is often measured
 108 by pass@ k , which describes the performance ceiling with k generations ([Chen et al., 2025b](#)).

More recently, scaling test-time compute via in-context “reasoning” (Brown et al., 2020; Wei et al., 2022) has significantly improved performance in domains like math and coding (Jaech et al., 2024). This capability is commonly enabled by large-scale, general-purpose RL training on diverse tasks (Lambert et al., 2025; Ma et al., 2025; Guo et al., 2025; Kimi et al., 2025), during which models learn to reason within their bounded context (Setlur et al., 2025b), which connects to the broad topic of meta-learning (Schmidhuber, 1987; Duan et al., 2017; Finn et al., 2017). **Curriculum learning, first proposed by Bengio et al. (2009), has been successfully applied to challenging RL problems (Sinapov et al., 2015; Narvekar et al., 2020).** This paradigm is closely related to goal-conditioned RL (Schaul et al., 2015; Andrychowicz et al., 2017) where several works have studied automatic curriculum generation (Florensa et al., 2018; Warde-Farley et al., 2018; Pitis et al., 2020; Pong et al., 2020). In contrast to improving general-purpose models, our work employs RL to train specialized reasoners for a particular target task at test-time.

Self-play. A specialized form of curriculum learning has proven highly successful in domains like games through the use of self-play (Schmidhuber, 1991; Silver et al., 2016), where an agent is repeatedly challenged by playing against itself. Seminal works show that this approach can lead to superhuman performance (e.g., Mnih et al., 2015; Silver et al., 2016; 2017; Berner et al., 2019). Several recent works aim to generalize this paradigm to LLMs and more general domains such as coding by self-generating a training curriculum (Zhao et al., 2025; Huang et al., 2025b; Chen et al., 2025a; Fang et al., 2025). While recent work has studied test-time curricula as an extension of self-play to goal-conditioned RL settings (Diaz-Bone et al., 2025), its evaluation has focused on simple robotic navigation tasks. We extend this line of work to challenging reasoning tasks by self-curating a training curriculum, enabling LLMs to continually learn from extensive experience on a single task (Silver & Sutton, 2025; Shen et al., 2025).

Test-time training and test-time RL. Training a model at test-time for a given input has been widely studied as TTT (Sun et al., 2020), using supervised (Hardt & Sun, 2024; Hübotter et al., 2025; Yu et al., 2025a; Bertolissi et al., 2025; Bagatella et al., 2025a) or self-supervised losses (Sun et al., 2025; Dalal et al., 2025). Several methods perform TTT in a purely unsupervised manner, i.e., without “real-world” data or feedback (Wang et al., 2021; Zhang et al., 2022). Most relevant to our work, Zuo et al. (2025) recently extended unsupervised TTT to perform RL on the test set, leveraging the model’s majority votes as pseudo-labels. This connects to a broader theme of unsupervised RL (Zhang et al., 2025a; Shao et al., 2025; Zhou et al., 2025; Prabhudesai et al., 2025) and self-improvement in LLMs (Zelikman et al., 2022; Gulcehre et al., 2023; Lee et al., 2025).

3 TEST-TIME CURRICULA

We consider the set of *target tasks* $\mathcal{D}^* = \{x_1^*, \dots, x_M^*\}$ given at test-time, and our goal is to specialize an existing model through further training to those tasks. For training, as in general-purpose RL, we rely on an existing large corpus of training tasks $\mathcal{D} = \{(x_i, v_i)\}_{i=1}^N$, for each of which $v_i(\cdot) \in \{0, 1\}$ verifies whether an attempt was correct. To specialize, it is common practice to construct a particular subset $\widehat{\mathcal{D}}^*$ from \mathcal{D} , and we call such a targeted subset a *test-time curriculum* for \mathcal{D}^* . We seek to make test-time training on such a curriculum scalable. To this end, we propose to go beyond human-curated test-time curricula and let the initial model craft its own test-time curriculum.

We propose a test-time curriculum agent, outlined in Algorithm 1. In each training step, the agent selects its next training task from the corpus \mathcal{D} based on its target tasks \mathcal{D}^* and the current model θ_{t-1} . This step leverages the semantic understanding of the model to *self-curate* a test-time curriculum for the target tasks. We then train on this test-time curriculum via GRPO (Shao et al., 2024).¹ Note that test-time training does not necessitate the model to stay

Algorithm 1 Test-Time Curriculum for Targeted RL

Require: Test tasks \mathcal{D}^*

```

1: for  $t = 1, 2, \dots, T$  do
2:    $(x_t, v_t) \leftarrow \text{TTC}_{\theta_{t-1}, \mathcal{D}}(\mathcal{D}^*)$             $\triangleright$  select next task
3:    $\{\hat{y}_{t,i}\} \sim \pi_{t-1}(\cdot | x_t)$                           $\triangleright$  attempt
4:    $\{r_{t,i}\} \leftarrow v_t(\{\hat{y}_{t,i}\})$                           $\triangleright$  verify
5:    $\theta_t \leftarrow \text{GRPO}(\theta_{t-1}, \{\hat{y}_{t,i}\}, \{r_{t,i}\})$      $\triangleright$  RL step
6: end for

```

¹Algorithm 1 abstracts that we perform each RL step over a batch of training tasks and that we perform RL training for multiple episodes.

162 close to its initialization since it needs to generalize only to its target tasks, and hence, we omit the
 163 KL penalty of GRPO. We include background on GRPO in Appendix B.
 164

165 While the previous works of Hardt & Sun (2024) and Hübotter et al. (2025) have studied self-curated
 166 test-time curricula with supervised fine-tuning (SFT) and shown that this can improve language
 167 modeling (i.e., lead to lower perplexity), we find that this approach does *not* improve accuracies
 168 on reasoning tasks. Perhaps counterintuitively, we find that test-time training with SFT—even on
 169 correct demonstrations of test tasks—can lead to an initial performance drop. Our findings mir-
 170 rror recent observations on the robustness of on-policy RL compared to off-policy SFT (Shenfeld
 171 et al., 2025). We provide further details in Appendix A. Moreover, while test-time training via SFT
 172 requires the corpus to specify *how* training tasks are to be solved, test-time training via RL only
 173 requires *verification* of solutions.

174 We next describe the corpus and TTC method used in our evaluation of the TTC-RL setting.

175 **An automatic TTC for targeted RL.** We adopt existing methods for TTC selection from previ-
 176 ous work studying test-time curricula with SFT (Hardt & Sun, 2024; Hübotter et al., 2025). These
 177 methods leverage a latent representation space ϕ over token sequences for which we use the nor-
 178 malized last-token last-layer embeddings of the initial model. We then utilize SIFT (Hübotter et al.,
 179 2025) which selects those examples from the corpus that the model deems most informative for the
 180 target tasks. SIFT has a hyperparameter λ which explicitly trades between diversity of the selected
 181 examples and their relevance to the target tasks. We find that our results are robust to the choice of
 182 λ and generally set $\lambda = 0.1$ in our experiments. Appendix F gives examples for such self-curated
 183 test-time curricula and we include background on SIFT in Appendix B.

184 The TTC selected by SIFT is static for given target tasks. Motivated by previous work on curricula
 185 for RL (e.g., Florensa et al., 2018; Narvekar et al., 2020; Pitis et al., 2020; Zhao et al., 2025) we also
 186 evaluate an adaptive curriculum that selects training tasks of appropriate difficulty for the current
 187 model. We find that this leads to diminishing returns if the corpus difficulty is already appropriately
 188 calibrated to the initial model, and therefore focus on the static curriculum in our main experiments.
 189 In Appendix C, we demonstrate that using a TTC of appropriately challenging training tasks, can
 190 significantly accelerate learning for a weaker initial model such as Qwen3-0.6B.

191 **A diverse corpus for general-purpose RL post-training.** To study the effectiveness of our pro-
 192 posed adaptive test-time curriculum, we leverage a large corpus of high-quality verifiable training
 193 data, suitable for post-training a model across diverse domains. We assemble a new meta-dataset,
 194 which we call the verifiable-corpus and which combines approximately 265k diverse training
 195 tasks, spanning three environments:

- 196 • **Exact answer match / Math:** For math problems with a numerical answer, we determine
 197 answer equivalence using `math-verify`. Our corpus contains the training splits of GSM8K
 198 (Cobbe et al., 2021) and MATH (Hendrycks et al., 2021b), and the DAPO math dataset (Yu
 199 et al., 2025b), covering numerically verifiable math problems for a wide range of difficulties.
- 200 • **Judged answer match / General reasoning:** Measuring the validity of complex reasoning
 201 requires more robust verification than symbolic equivalence checks. Given a (potentially
 202 long) golden answer, we use a 1.5B-parameter verifier model trained by Ma et al. (2025) to
 203 determine whether attempted and golden answers are semantically equivalent. Our corpus
 204 contains the Webinstruct-verified dataset (Ma et al., 2025), which covers a wide variety of
 205 subjects ranging from natural sciences to history.
- 206 • **Unit tests / Code:** Finally, we combine several sources of coding tasks. Each coding task
 207 is verified by a set of unit tests. Our corpus combines tasks from APPS (Hendrycks et al.,
 208 2021a), code contests (Li et al., 2022), TACO (Li et al., 2023), PrimeIntellect (Mattern et al.,
 209 2025), Leetcode (Xia et al., 2025), the Codeforces training split (Penedo et al., 2025) and all
 210 LiveCodeBench tasks (Jain et al., 2025) prior to February 1, 2025.

211 We perform a filtering step where we remove training tasks with empty answers or less than 5 unit
 212 tests, to ensure a reliable training signal. Finally, we deduplicate and decontaminate the corpus,
 213 as detailed in Appendix E.1. We openly share the corpus and our environment implementations
 214 to support future research. To our knowledge, the verifiable-corpus is one of the first public
 215 corpora of high-quality verifiable tasks, spanning several domains and environments. We envision
 that, building on this work, future efforts will ultimately enable TTC agents to utilize any relevant

Model	AIME24	AIME25	MATH500	Codeforces	CodeElo	LCB ^{v6}	GPQA-D
Qwen3-8B	21.67	23.33	69.55	20.85	13.73	20.61	49.11
+ RL post-training	41.67	38.33	82.50	27.83	22.67	25.95	56.47
+ TTC-RL	50.83 ^{+29.2}	41.67 ^{+18.3}	85.10 ^{+15.6}	33.35 ^{+12.5}	29.34 ^{+15.6}	27.29 ^{+6.7}	58.38 ^{+9.3}
Qwen3-4B-Instruct-2507	52.50	40.83	72.00	26.70	20.27	21.56	61.93
+ RL post-training	55.83	47.50	86.30	28.39	21.18	25.95	62.82
+ TTC-RL	60.00 ^{+7.5}	45.83 ^{+5.0}	88.50 ^{+16.5}	34.99 ^{+8.3}	27.20 ^{+6.9}	26.91 ^{+5.4}	61.93 ^{+0.0}
Qwen3-8B-Base	15.83	14.17	63.10	9.92	6.67	11.26	29.70
+ RL post-training	22.50	20.83	76.85	17.46	9.97	18.51	42.77
+ TTC-RL	30.00 ^{+14.2}	21.67 ^{+7.5}	78.15 ^{+15.1}	17.84 ^{+7.9}	11.33 ^{+4.7}	17.94 ^{+6.7}	45.94 ^{+16.2}

Table 1: **Performance of TTC-RL on reasoning benchmarks.** We evaluate TTC-RL across benchmarks for math (AIME24, AIME25, MATH500), coding (Codeforces, CodeElo, LCB^{v6}), and scientific reasoning (GPQA-D). Numbers in **bold** denote the best performance for a given model backbone, and we use ⁺ to denote the improvement over the initial model in percentage points.

training tasks they find on the web (similarly to retrieval-augmented generation; Lewis et al., 2019), or to self-generate their own training tasks (see, e.g., Zhao et al., 2025).

4 RESULTS

We focus our evaluation on a diverse set of target tasks in math, coding, and scientific reasoning. Specifically, we evaluate test-time curricula for high-school-level competition math questions in AIME 24 & 25 and MATH500 (Hendrycks et al., 2021b). We evaluate coding ability on Codeforces (Penedo et al., 2025), CodeElo (Quan et al., 2025), and on LiveCodeBench v6 (Jain et al., 2025), i.e., tasks released after February 1, 2025. Finally, we evaluate scientific reasoning with GPQA-Diamond (Rein et al., 2024) which covers questions in biology, physics, and chemistry.

TTC-RL can be applied to each task within a benchmark individually or to the entire benchmark on aggregate, treating it as a set of target tasks. We primarily evaluate TTC-RL per-benchmark as this yields greater statistical significance under a limited compute budget. We then perform an ablation, indicating that per-task TTCs performs at least on-par with per-benchmark TTCs (cf. Section 4.2).

To ensure that our evaluation is accurate, we adopt evalchemy (Raoof et al., 2025) and synthesize system prompts to be consistent across benchmarks (cf. Appendix E.2). We generally train for two episodes with batch size 8 and 16 rollouts per train task,² and measure avg@4 on the set of test tasks once every ten steps. To further reduce noise, we compute a moving average across three validation steps. Finally, in our summarized numeric results, we report the highest averaged avg@4, and include detailed plots of avg@4 per step in Appendix D.2.

We perform our main evaluation on the non-thinking models Qwen3-8B (Yang et al., 2025) and the more recent Qwen3-4B-Instruct-2507, whose responses we limit to 8192 tokens. We additionally evaluate on the Qwen3-8B base model. We opt for non-thinking models due to the high computational cost of running thinking models over long contexts, typically of up to 32k tokens. The goal of our TTC framework is to show that models can improve at test-time, even without further expanding their context. We hypothesize that our results extend to thinking models, which simply have a larger maximum response length.

Main results. We summarize our main results in Figure 1 and Table 1. We find that TTC-RL significantly improves accuracy across a range of models and all benchmarks. Notably, it also leads to significant performance gains on top of Qwen3-8B-Base within only relatively few RL steps, indicating that TTCs lead to sample-efficient training. Our main baseline is a model that is trained on 1k uniformly chosen training tasks from the corpus, to which we refer to as standard “RL post-training”, since this method yields a general-purpose model. We compare this to TTC-RL with a curriculum of size 1k and find that training on a test-time curriculum accelerates learning significantly and leads to

²We summarize all training hyperparameters in Appendix E.3.

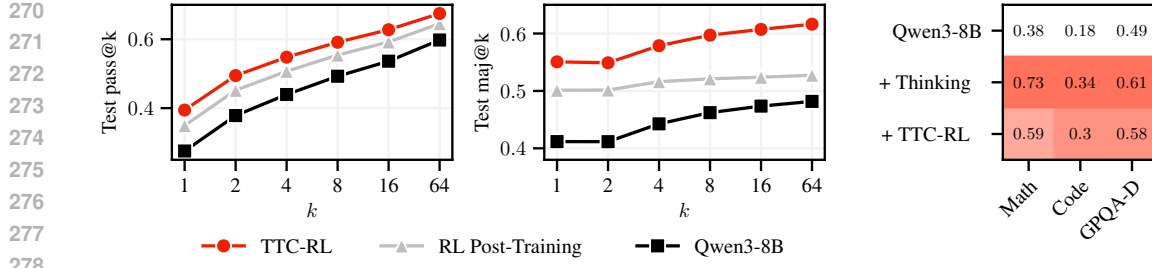


Figure 3: **TTC-RL scales test-time compute in way that is complementary to other means of test-time scaling.** **Left:** The pass@ k of TTC-RL on Qwen3-8B, averaged over benchmarks, increases substantially for small and large k , indicating that TTC-RL raises the model’s performance ceiling. **Middle:** TTC-RL also improves the performance of majority voting (across math and GPQA-D), with the initial pass@1 significantly outperforming maj@64 on the initial model. **Right:** We evaluate Qwen3-8B in non-thinking and thinking mode, as well as the non-thinking model + TTC-RL. The color indicates the relative accuracy per column. We find that TTC-RL significantly improves the non-thinking model, allowing it to perform close to the thinking variant in several domains, despite reasoning over 8k rather than 30k context tokens.

saturation at substantially higher performance.³ Notably, Qwen3-8B with TTC-RL performs on-par with strong closed-source non-thinking models; for example, it approximately matches GPT-4o-2024-08-06 on LCB^{v6} and outperforms GPT 4.1 and Claude Opus 4.1 on AIME.

In Figure 2, we further ablate the size of the curriculum and find that TTC-RL consistently outperforms general-purpose RL post-training across a wide range of curriculum sizes. Interestingly, at dataset size 1—though performing poorly—the general-purpose RL post-training outperforms TTC-RL. We suspect that this may result from TTC-RL picking a practice task that is very similar to the test tasks, in which case overfitting may harm more than when overfitting to a less related task.

Takeaway 1

TTC-RL substantially improves accuracy on a wide variety of models and benchmarks, compared to a model’s initial performance and after (continued) RL post-training on our corpus.

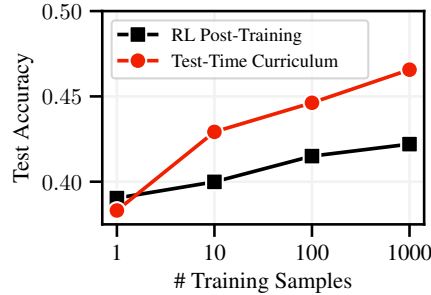


Figure 2: **TTC-RL outperforms RL post-training across data sizes.** We evaluate Qwen3-8B on all seven benchmarks and report the average test accuracy when training for 250 steps.

4.1 TTCS ARE COMPLEMENTARY TO EXISTING APPROACHES TO TEST-TIME SCALING

Next, we demonstrate that TTC-RL *improves* the LLM’s ability for test-time scaling.

TTCS raise the model’s performance ceiling. While the improvement in accuracy demonstrates that during TTC-RL, the model learns to better reason within context, we ask whether the model improves more broadly. A common metric to understand a model’s “performance ceiling” for test-time scaling is the pass@ k metric, which measures whether any one of k attempts is correct (Chen et al., 2025b). Recent work has repeatedly shown that RL-training tends not to improve pass@ k at large k (Yue et al., 2025), leading to the concern that RL-training is simply “distilling” pass@ k into pass@1. In Figure 3 (left), we instead observe that TTC-RL significantly improves pass@ k across a wide range of k . Similarly, TTC-RL also improves the realized performance gains of majority voting, as can be seen in Figure 3 (middle), and notably increases the pass@1 well beyond the maj@64 after continued RL post-training. Since RL post-training and TTC-RL differ only in their training tasks, our results demonstrate that targeted selection of training tasks can lead to

³In Appendix D.3, we additionally compare to an “RL post-training” baseline that only samples training tasks from the test environment and show that this yields comparable results.

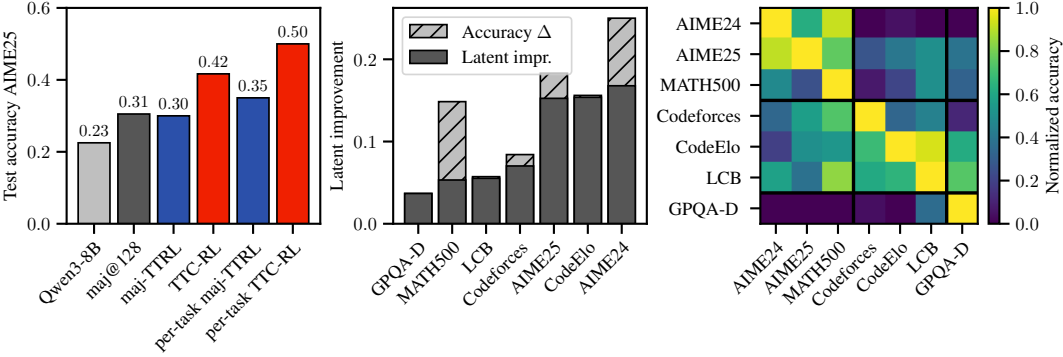


Figure 4: **Left: Per-task TTC-RL outperforms a benchmark-level TTC in AIME25.** We perform TTC-RL and maj-TTRL (cf. Section 5.2) on Qwen3-8B, and find that per-task TTC-RL even outperforms the benchmark-level TTC. **Middle: TTC-RL improves “correctness” of reasoning, not only learning the answer format.** We evaluate the difference in accuracy between TTC-RL and the initial Qwen3-8B, averaged over benchmarks. The latent improvement is a lower bound on the accuracy gain that is not due to merely learning the format (cf. Section 5.1). **Right: TTC-RL yields models that are specialized to their target tasks.** We plot the accuracy of Qwen3-8B trained for given target tasks (rows) when evaluated on other benchmarks (columns). We normalize accuracies across all evaluations of a particular benchmark. Notably, the model trained via TTC-RL for the “right” target tasks (i.e., the diagonal) always performs best.

substantial performance gains. Furthermore, we find that increasing clip-high in GRPO as proposed by Yu et al. (2025b) improves exploration and prevents entropy collapse in RL post-training as well as TTC-RL (cf. Appendix D.1), which is crucial for improving upon the strong initial models. Developing a better understanding of the circumstances under which RL-training can “discover new behavior”, leading to improved pass@ k , is an exciting direction for future research.

TTC-RL with a short-context LLM can perform close to a long-context LLM. We also seek to better understand how TTC-RL relates to reasoning over long contexts. To this end, we evaluate the non-thinking and thinking variants of Qwen3-8B, limited to 8k and 30k tokens per response, respectively. In Figure 3 (right), we find that TTC-RL on the non-thinking model performs close to the thinking model in several domains, particularly in coding and GPQA.⁴ Further, note that the asymptotic cost of growing context in a Transformer is quadratic (Vaswani et al., 2017), whereas the asymptotic cost of TTC-RL is linear (since experience is compressed into the model’s weights). This suggests that there is a regime in which, given a fixed compute budget, TTC-RL outperforms further scaling of context size. We believe that studying this compute-optimal Pareto frontier is an exciting topic for future research. Our results indicate that to further improve the performance of LLMs, test-time curricula may eventually be advantageous over continued scaling of context size.

Takeaway 2

Test-time curricula substantially increase the pass@ k performance ceiling of a model and can perform similarly to models which are reasoning over a much larger context. This indicates the potential of TTCs to complement existing approaches to test-time scaling.

4.2 TTCs EFFECTIVELY SPECIALIZE MODELS

To determine whether the test-time curriculum specializes the model to its target tasks, we conduct a straightforward experiment: We evaluate each final checkpoint of TTC-RL on all benchmarks, including those that were not part of the set of target tasks. We summarize the results in Figure 4 (right), with columns corresponding to evaluation and rows corresponding to training. We find that after TTC-RL, models perform best on their target tasks, while severely underperforming on tasks that are unrelated to the target tasks. Moreover, we identify a block-diagonal structure, where models generalize better across mutually related groups of tasks, particularly among similar math

⁴In MATH500, non-thinking Qwen3-8B + TTC-RL (85%) even outperformed the thinking variant (77%).

378 benchmarks. We also find that models appear to generalize better from coding to math than vice
 379 versa, and models generalize better from code and math to GPQA than vice versa.
 380

381 **TTCs for individual tasks.** Aspirationally, we anticipate test-time curricula to enable continual
 382 learning for a single test task over a long timeframe. While we focus our main evaluation on the
 383 setting where test-time curricula are applied per benchmark, we run an ablation with 30 separate
 384 TTCs—one per AIME 25 question. The results in Figure 4 (left) demonstrate that *specializing* to an
 385 individual test task can outperform a broader specialization to a group of test tasks. This shows that
 386 TTC-RL does not depend on a larger set of test tasks to implicitly lead to diverse data and robust
 387 training, and instead seamlessly extends to a fully test-time setting with only a single task given.
 388 We find, however, that more fine-grained specialization does not always lead to further performance
 389 gains. We evaluate training separate TTCs for each of biology, physics, and chemistry in GPQA,
 390 leading to approximately the same performance as a joint TTC. In our view, gaining a better
 391 understanding for “how much” specialization is helpful is an exciting direction for further research.
 392

393 **Takeaway 3**

394 Test-time curricula effectively specialize the model to their target tasks. When applied to an
 395 individual target task, TTC-RL can be seen directly as a method for test-time scaling.

396

5 FURTHER ANALYSIS

397

5.1 ESTIMATING “REAL” IMPROVEMENT

401 When evaluating RL-trained models on verifiable tasks, a reasonable concern is whether the
 402 model simply learns to adhere to the expected output format. Indeed, we find that if the initial
 403 model is not able to consistently produce well-formed responses, RL-training tends to quickly
 404 teach the model the expected output format. Therefore, disentangling shallow learning of format
 405 from improvements in a model’s “latent” reasoning is critical for accurate evaluation. Ideally, we
 406 would like to measure whether the model’s reasoning improves throughout training—regardless of
 407 whether we can automatically parse and evaluate responses.

408 We propose to measure a model’s *latent improvement* (LI) during RL training as follows. Consider
 409 the event of an answer being marked as “accurate” by the verifier, which occurs if it is “well-formed”
 410 (i.e., it can be extracted and interpreted) and if the model’s latent reasoning is “correct”. Based on
 411 this, a straightforward lower bound on correctness is simply $\mathbb{P}(\text{correct}) \geq \mathbb{P}(\text{accurate})$. To measure the
 412 *improvement* in correctness throughout RL training, we make the following intuitive assumption:

413 **Assumption 1.** *We assume that being well-formed does not reduce the chance of being correct.*
 414 *Formally, we assume $\mathbb{P}(\text{correct} \mid \text{well-formed}) \geq \mathbb{P}(\text{correct})$, i.e., a non-negative association of*
 415 *formedness and correctness.*

416 Intuitively, this assumption states that an *ill-formed response does not increase the likelihood of*
 417 *correct latent reasoning*. This yields a straightforward upper bound on the probability of correct
 418 latent reasoning: $\mathbb{P}(\text{correct}) \leq \mathbb{P}(\text{accurate})/\mathbb{P}(\text{well-formed})$ if $\mathbb{P}(\text{well-formed}) > 0$. Thus, the
 419 improvement in correctness after T RL steps is lower bounded as

$$420 \text{Latent Improvement} := \mathbb{P}(\text{correct}_T) - \mathbb{P}(\text{correct}_0) \geq \mathbb{P}(\text{accurate}_T) - \frac{\mathbb{P}(\text{accurate}_0)}{\mathbb{P}(\text{well-formed}_0)}. \quad (1)$$

423 **Measuring latent improvement.** We consider a response as ill-formed if we cannot extract an
 424 answer, e.g., because the response was truncated at the max-token limit or because the completed
 425 response did not contain an extractable answer. We note that to reliably measure LI, it is essential
 426 to ensure that answer extraction is strict.⁵ In Figure 4 (middle), we measure the latent improvement
 427 of Qwen3-8B, and find that under Assumption 1, TTC-RL leads to a substantial latent improvement.
 428 We include our complete results in terms of LI in Table 7 of Appendix D.
 429

430 ⁵If answers are extracted, which are not intended as answers by the model, this artificially inflates LI and
 431 violates Assumption 1. To ensure this, we only extract the contents of `\boxed{}` or the contents wrapped in “` “`
 for math and code, respectively.

432 5.2 TOWARDS CONTINUAL SELF-IMPROVEMENT AT TEST-TIME
433

434 We consider this work as a first step towards agents that continue learning at test-time and specialize
435 without requiring human supervision. The recent work of Zuo et al. (2025) can also be seen as a
436 step in this direction by proposing to train on the test set directly, using majority votes as surrogate
437 rewards (“maj-TTRL”). Since Maj-TTRL relies on majority votes as its training signal, it can be
438 applied only to environments with structured outputs such as our math environment with numerical
439 answers or the multiple choice GPQA. In contrast, our proposed TTCs can be applied in any
440 environment where a reward signal can be defined. We perform a comparison to Zuo et al. (2025) in
441 Table 2 and find that Maj-TTRL leads to significant gains in accuracy across math benchmarks, but
442 helping less in GPQA. We emphasize that Maj-TTRL and test-time curricula are complementary
443 approaches, e.g., one can perform Maj-TTRL directly after TTC-RL, which we find to outperform
444 Maj-TTRL alone (cf. Figure 11 in Appendix D.4).

445 Notably, the performance gains of Maj-TTRL on the
446 strong Qwen3-4B-Instruct-2507 model in AIME 24 &
447 25 suggest that the returns from our proposed imple-
448 mentation of TTC-RL are constrained by the scope of its
449 fixed training corpus. This saturation does not imply a
450 ceiling on the model’s capabilities; rather, it may indicate
451 a promising opportunity for self-improvement methods
452 such as Maj-TTRL or synthetic data generation (e.g.,
453 Zhao et al., 2025; Zweiger et al., 2025), which may be
454 combined with or extend TTCs.

455 5.3 ON CONTAMINATION AND REWARD HACKING
456

457 The performance gains from TTC-RL are remarkable: for
458 example, in AIME24 and CodeElo, the pass@1 of the
459 strong Qwen3-8B more than doubles within only a few
460 hundred training steps. This naturally raises the question
461 of potential confounding factors. To mitigate this risk, we took several steps: we extensively de-
462 contaminated our corpus by removing tasks that overlap with the test sets, implemented safeguards
463 against reward hacking within our code environment, and manually reviewed several model re-
464 sponses. While we base our evaluation on the widely used evalchem package (Raoof et al., 2025),
465 we found a significant flaw in the evaluation of Codeforces and CodeElo, where some (and fre-
466 quently all) private test cases were leaked into the prompt as “examples”. This enables a strong
467 model to “solve” a task simply by handling each test case individually. To mitigate this, we re-
468 moved all input/output examples from the prompts of Codeforces and CodeElo, and also ensured
469 that private test cases are not leaked in tasks from our training corpus.

470 A remaining limitation is that we cannot guarantee the cleanliness of the model’s original pre-
471 training data. To account for this possibility, we evaluate on LCB^{v6}, which consists of coding
472 tasks that were released since February 2025. Hence, TTC-RLs performance gains on LCB makes
473 pre-existing contamination a less likely explanation for our results. Furthermore, we compare TTC-
474 RL to an oracle that trains directly on the test tasks, finding that our method learns slightly more
475 slowly and levels off at a lower accuracy (cf. Figure 13 in Appendix D). We believe our findings
476 on the importance of data selection (cf. Figure 1) and improvements to the RL training algorithm to
477 facilitate exploration (cf. Appendix D.1) offer plausible explanations for these results. We further
478 include qualitative examples demonstrating the improvements in reasoning in Appendix F.

480 6 DISCUSSION
481

482 We propose a test-time curriculum agent that self-curates a sequence of training tasks to specialize
483 towards a specific target task via reinforcement learning. We demonstrate that TTCs achieve
484 remarkable performance gains across multiple models and diverse reasoning benchmarks, sig-
485 nificantly raising the performance ceiling of strong initial models through specialization to their
target task. To better evaluate these gains, we introduce the “latent improvement” metric, which

Model	Math	Code	GPQA-D
Qwen3-8B-Instruct			
+ Maj-TTRL	52.63	–	51.14
+ TTC-RL	59.2	29.99	58.38
Qwen3-4B-Instruct-2507			
+ Maj-TTRL	69.49	–	62.44
+ TTC-RL	64.78	29.70	61.93

Table 2: The competitive performance of Maj-TTRL on our strongest model suggests that TTC-RL’s effectiveness is constrained by its fixed training corpus. Combining our approach with self-improvement techniques is therefore an exciting direction for future work.

486 measures genuine improvements in reasoning correctness. Our experiments confirm that TTCs
 487 yield substantial gains in latent improvement.
 488

489 This highlights the potential of a currently underutilized compute regime: targeted test-time training,
 490 which sits between large-scale general-purpose training and frozen test-time scaling. While standard
 491 next-token prediction relies on a model’s intuition and reasoning allows it to leverage context for
 492 deliberation, our proposed test-time curriculum enables the model to meta-learn *how* to reason for a
 493 particular target task at test-time. Similarly, when humans begin a new job, they often train for weeks
 494 or months before being able to solve all required tasks. During this time, they collect experience on
 495 dozens of tasks that are similar, becoming more efficient at solving their jobs’ target tasks.
 496

497 In demonstrating the potential of such targeted test-time training, our work opens up several exciting
 498 research directions. A natural direction is to move beyond the bottleneck of a fixed task corpus
 499 through self-generated TTCs, which may still use human-created tasks as inspiration. Further
 500 avenues include improving the sample- and step-efficiency of TTC-RL through advancing methods for
 501 RL training. This also raises questions about scaling laws for this new regime: for instance, at what
 502 context length does it become more advantageous to scale TTC-RL rather than increasing the context
 503 window? Looking beyond single-task specialization, TTCs might be extended to dynamic settings
 504 where an agent must adapt to an evolving set of target tasks. Finally, TTC-RL could be used to un-
 505 confound benchmark evaluations by providing a standardized method for specializing all models to
 506 a test task (Dominguez-Olmedo et al., 2025), enabling a fairer comparison of their core capabilities.
 507

508 REFERENCES

509 Ekin Akyürek, Mehul Damani, Adam Zweiger, Linlu Qiu, Han Guo, Jyothish Pari, Yoon Kim, and
 510 Jacob Andreas. The surprising effectiveness of test-time training for few-shot learning. In *ICML*,
 511 2025.

512 Marcin Andrychowicz, Filip Wolski, Alex Ray, Jonas Schneider, Rachel Fong, Peter Welinder, Bob
 513 McGrew, Josh Tobin, Pieter Abbeel, and Wojciech Zaremba. Hindsight experience replay. In
 514 *NeurIPS*, 2017.

515 Marco Bagatella, Mert Albaba, Jonas Hübotter, Georg Martius, and Andreas Krause. Test-time of-
 516 fline reinforcement learning on goal-related experience. *arXiv preprint arXiv:2507.18809*, 2025a.

517 Marco Bagatella, Jonas Hübotter, Georg Martius, and Andreas Krause. Active fine-tuning of multi-
 518 task policies. In *ICML*, 2025b.

519 Yoshua Bengio, Jérôme Louradour, Ronan Collobert, and Jason Weston. Curriculum learning. In
 520 *ICML*, 2009.

521 Christopher Berner, Greg Brockman, Brooke Chan, Vicki Cheung, Przemysław Debiak, Christy
 522 Dennison, David Farhi, Quirin Fischer, Shariq Hashme, Chris Hesse, et al. Dota 2 with large
 523 scale deep reinforcement learning. *arXiv preprint arXiv:1912.06680*, 2019.

524 Ryo Bertolissi, Jonas Hübotter, Ido Hakimi, and Andreas Krause. Local mixtures of experts: Essen-
 525 tially free test-time training via model merging. In *COLM*, 2025.

526 Tom B. Brown, Benjamin Mann, Nick Ryder, Melanie Subbiah, Jared Kaplan, Prafulla Dhariwal,
 527 Arvind Neelakantan, Pranav Shyam, Girish Sastry, Amanda Askell, et al. Language models are
 528 few-shot learners. *arXiv preprint ArXiv:2005.14165*, 2020.

529 Lili Chen, Mihir Prabhudesai, Katerina Fragkiadaki, Hao Liu, and Deepak Pathak. Self-questioning
 530 language models. *arXiv preprint arXiv:2508.03682*, 2025a.

531 Mark Chen, Jerry Tworek, Heewoo Jun, Qiming Yuan, Henrique Ponde De Oliveira Pinto, Jared
 532 Kaplan, Harri Edwards, Yuri Burda, Nicholas Joseph, Greg Brockman, et al. Evaluating large
 533 language models trained on code. *arXiv preprint arXiv:2107.03374*, 2021.

534 Zhipeng Chen, Xiaobo Qin, Youbin Wu, Yue Ling, Qinghao Ye, Wayne Xin Zhao, and Guang Shi.
 535 Pass@k training for adaptively balancing exploration and exploitation of large reasoning models.
 536 *arXiv preprint arXiv:2508.10751*, 2025b.

540 Karl Cobbe, Vineet Kosaraju, Mohammad Bavarian, Mark Chen, Heewoo Jun, Lukasz Kaiser,
 541 Matthias Plappert, Jerry Tworek, Jacob Hilton, Reiichiro Nakano, et al. Training verifiers to
 542 solve math word problems. *arXiv preprint arXiv:2110.14168*, 2021.

543

544 Karan Dalal, Daniel Koceja, Gashon Hussein, Jiarui Xu, Yue Zhao, Youjin Song, Shihao Han,
 545 Ka Chun Cheung, Jan Kautz, Carlos Guestrin, et al. One-minute video generation with test-time
 546 training. In *CVPR*, 2025.

547 Leander Diaz-Bone, Marco Bagatella, Jonas Hübotter, and Andreas Krause. Discover: Automated
 548 curricula for sparse-reward reinforcement learning. In *NeurIPS*, 2025.

549

550 Ricardo Dominguez-Olmedo, Florian E Dorner, and Moritz Hardt. Training on the test task con-
 551 founders evaluation and emergence. In *ICLR*, 2025.

552 Yan Duan, John Schulman, Xi Chen, Peter L Bartlett, Ilya Sutskever, and Pieter Abbeel. Rl²: Fast
 553 reinforcement learning via slow reinforcement learning. In *ICLR*, 2017.

554

555 Wenkai Fang, Shunyu Liu, Yang Zhou, Kongcheng Zhang, Tongya Zheng, Kaixuan Chen, Mingli
 556 Song, and Dacheng Tao. Serl: Self-play reinforcement learning for large language models with
 557 limited data. In *NeurIPS*, 2025.

558 Chelsea Finn, Pieter Abbeel, and Sergey Levine. Model-agnostic meta-learning for fast adaptation
 559 of deep networks. In *ICML*, 2017.

560

561 Carlos Florensa, David Held, Xinyang Geng, and Pieter Abbeel. Automatic goal generation for
 562 reinforcement learning agents. In *ICML*, 2018.

563

564 Etash Guha, Ryan Marten, Sedrick Keh, Negin Raoof, Georgios Smyrnis, Hritik Bansal, Marianna
 565 Nezhurina, Jean Mercat, Trung Vu, Zayne Sprague, et al. Openthoughts: Data recipes for reason-
 566 ing models. *arXiv preprint arXiv:2506.04178*, 2025.

567

568 Caglar Gulcehre, Tom Le Paine, Srivatsan Srinivasan, Ksenia Konyushkova, Lotte Weerts, Abhishek
 569 Sharma, Aditya Siddhant, Alex Ahern, Miaosen Wang, Chenjie Gu, et al. Reinforced self-training
 (rest) for language modeling. *arXiv preprint arXiv:2308.08998*, 2023.

570

571 Daya Guo, Dejian Yang, Haowei Zhang, Junxiao Song, Ruoyu Zhang, Runxin Xu, Qihao Zhu,
 572 Shirong Ma, Peiyi Wang, Xiao Bi, et al. Deepseek-r1: Incentivizing reasoning capability in llms
 573 via reinforcement learning. *arXiv preprint arXiv:2501.12948*, 2025.

574

575 Moritz Hardt and Yu Sun. Test-time training on nearest neighbors for large language models. In
 576 *ICLR*, 2024.

577

578 Dan Hendrycks, Steven Basart, Saurav Kadavath, Mantas Mazeika, Akul Arora, Ethan Guo, Collin
 579 Burns, Samir Puranik, Horace He, Dawn Song, and Jacob Steinhardt. Measuring coding challenge
 competence with apps. In *NeurIPS*, 2021a.

580

581 Dan Hendrycks, Collin Burns, Saurav Kadavath, Akul Arora, Steven Basart, Eric Tang, Dawn
 582 Song, and Jacob Steinhardt. Measuring mathematical problem solving with the math dataset.
 In *NeurIPS*, 2021b.

583

584 Audrey Huang, Adam Block, Dylan J Foster, Dhruv Rohatgi, Cyril Zhang, Max Simchowitz, Jor-
 585 dan T Ash, and Akshay Krishnamurthy. Self-improvement in language models: The sharpening
 586 mechanism. In *ICLR*, 2025a.

587

588 Chengsong Huang, Wenhao Yu, Xiaoyang Wang, Hongming Zhang, Zongxia Li, Ruosen Li, Jiaxin
 589 Huang, Haitao Mi, and Dong Yu. R-zero: Self-evolving reasoning llm from zero data. *arXiv
 preprint arXiv:2508.05004*, 2025b.

590

591 Jonas Hübotter, Bhavya Sukhija, Lenart Treven, Yarden As, and Andreas Krause. Transductive
 592 active learning: Theory and applications. In *NeurIPS*, 2024.

593

Jonas Hübotter, Sascha Bongni, Ido Hakimi, and Andreas Krause. Efficiently learning at test-time:
 Active fine-tuning of llms. In *ICLR*, 2025.

594 Aaron Jaech, Adam Kalai, Adam Lerer, Adam Richardson, Ahmed El-Kishky, Aiden Low, Alec
 595 Helyar, Aleksander Madry, Alex Beutel, Alex Carney, et al. Openai o1 system card. *arXiv*
 596 *preprint arXiv:2412.16720*, 2024.

597 Naman Jain, King Han, Alex Gu, Wen-Ding Li, Fanjia Yan, Tianjun Zhang, Sida Wang, Armando
 598 Solar-Lezama, Koushik Sen, and Ion Stoica. Livecodebench: Holistic and contamination free
 599 evaluation of large language models for code. In *ICLR*, 2025.

600 Kimi, Angang Du, Bofei Gao, Bowei Xing, Changjiu Jiang, Cheng Chen, Cheng Li, Chenjun Xiao,
 601 Chenzhuang Du, Chonghua Liao, et al. Kimi k1.5: Scaling reinforcement learning with llms.
 602 *arXiv preprint arXiv:2501.12599*, 2025.

603 Nathan Lambert, Jacob Morrison, Valentina Pyatkin, Shengyi Huang, Hamish Ivison, Faeze Brah-
 604 man, Lester James V Miranda, Alisa Liu, Nouha Dziri, Shane Lyu, et al. Tulu 3: Pushing frontiers
 605 in open language model post-training. In *COLM*, 2025.

606 Nayoung Lee, Ziyang Cai, Avi Schwarzschild, Kangwook Lee, and Dimitris Papailiopoulos. Self-
 607 improving transformers overcome easy-to-hard and length generalization challenges. In *ICML*,
 608 2025.

609 Patrick Lewis, Ethan Perez, Aleksandra Piktus, Fabio Petroni, Vladimir Karpukhin, Naman Goyal,
 610 Heinrich Kütller, Mike Lewis, Wen-tau Yih, Tim Rocktäschel, et al. Retrieval-augmented gener-
 611 ation for knowledge-intensive nlp tasks. In *NeurIPS*, 2019.

612 Rongao Li, Jie Fu, Bo-Wen Zhang, Tao Huang, Zhihong Sun, Chen Lyu, Guang Liu, Zhi Jin, and
 613 Ge Li. Taco: Topics in algorithmic code generation dataset. *arXiv preprint arXiv:2312.14852*,
 614 2023.

615 Yujia Li, David Choi, Junyoung Chung, Nate Kushman, Julian Schrittwieser, Rémi Leblond, Tom
 616 Eccles, James Keeling, Felix Gimeno, Agustin Dal Lago, et al. Competition-level code generation
 617 with alphacode. *arXiv preprint arXiv:2203.07814*, 2022.

618 Hunter Lightman, Vineet Kosaraju, Yuri Burda, Harrison Edwards, Bowen Baker, Teddy Lee, Jan
 619 Leike, John Schulman, Ilya Sutskever, and Karl Cobbe. Let's verify step by step. In *ICLR*, 2023.

620 Michael Luo, Sijun Tan, Roy Huang, Ameen Patel, Alpay Ariyak, Qingyang Wu, Xiaoxiang Shi,
 621 Rachel Xin, Colin Cai, Maurice Weber, et al. Deepcoder: A fully open-source 14b coder at
 622 o3-mini level. *Together AI Blog*, 2025. URL <https://www.together.ai/blog/deepcoder>.

623 Xueguang Ma, Qian Liu, Dongfu Jiang, Ge Zhang, Zejun Ma, and Wenhui Chen. General-reasoner:
 624 Advancing llm reasoning across all domains. In *NeurIPS*, 2025.

625 David JC MacKay. Information-based objective functions for active data selection. *Neural computa-
 626 tion*, 4(4), 1992.

627 Justus Mattern, Manveer, Jannik, Matthew, Felix, Johannes, and Vincent. Synthetic-1: Scaling
 628 distributed synthetic data generation for verified reasoning. *PrimeIntellect Blog*, 2025. URL
 629 <https://www.primeintellect.ai/blog/synthetic-1>.

630 Volodymyr Mnih, Koray Kavukcuoglu, David Silver, Andrei A. Rusu, Joel Veness, Marc G. Belle-
 631 mare, Alex Graves, Martin Riedmiller, Andreas K. Fidjeland, Georg Ostrovski, et al. Human-level
 632 control through deep reinforcement learning. *Nature*, 518(7540), 2015.

633 Sanmit Narvekar, Bei Peng, Matteo Leonetti, Jivko Sinapov, Matthew E. Taylor, and Peter Stone.
 634 Curriculum learning for reinforcement learning domains: A framework and survey. *JMLR*, 2020.

635 Guilherme Penedo, Anton Lozhkov, Hynek Kydlíček, Loubna Ben Allal, Edward Beeching,
 636 Agustín Piquerres Lajarín, Quentin Gallouédec, Nathan Habib, Lewis Tunstall, and Leandro
 637 von Werra. Codeforces dataset, 2025. URL [codeforces](https://huggingface.co/datasets/open-r1/

 638 <a href=).

639 Silviu Pitis, Harris Chan, Stephen Zhao, Bradly Stadie, and Jimmy Ba. Maximum entropy gain
 640 exploration for long horizon multi-goal reinforcement learning. In *ICML*, 2020.

648 Vitchyr H. Pong, Murtaza Dalal, Steven Lin, Ashvin Nair, Shikhar Bahl, and Sergey Levine. Skew-
 649 fit: State-covering self-supervised reinforcement learning. In *ICML*, 2020.

650

651 Mihir Prabhudesai, Lili Chen, Alex Ippoliti, Katerina Fragkiadaki, Hao Liu, and Deepak Pathak.
 652 Maximizing confidence alone improves reasoning. *arXiv preprint arXiv:2505.22660*, 2025.

653

654 Shanghaoran Quan, Jiaxi Yang, Bowen Yu, Bo Zheng, Dayiheng Liu, An Yang, Xuancheng Ren,
 655 Bofei Gao, Yibo Miao, Yunlong Feng, et al. Codeelo: Benchmarking competition-level code
 656 generation of llms with human-comparable elo ratings. *arXiv preprint arXiv:2501.01257*, 2025.

657

658 Qwen. Qwq-32b: Embracing the power of reinforcement learning. *Qwen Blog*, 2025. URL <https://qwenlm.github.io/blog/qwq-32b>.

659

660 Qwen, An Yang, Baosong Yang, Beichen Zhang, Binyuan Hui, Bo Zheng, Bowen Yu, Chengyuan
 661 Li, Dayiheng Liu, Fei Huang, et al. Qwen2.5 technical report. *arXiv preprint arXiv:2412.15115*,
 662 2024.

663

664 Negin Raoof, Etash Kumar Guha, Ryan Marten, Jean Mercat, Eric Frankel, Sedrick Keh, Hritik
 665 Bansal, Georgios Smyrnis, Marianna Nezhurina, Trung Vu, et al. Evalchemy, 2025.

666

667 David Rein, Betty Li Hou, Asa Cooper Stickland, Jackson Petty, Richard Yuanzhe Pang, Julien Di-
 668 rani, Julian Michael, and Samuel R Bowman. Gpqa: A graduate-level google-proof q&a bench-
 669 mark. In *COLM*, 2024.

670

671 Tom Schaul, Daniel Horgan, Karol Gregor, and David Silver. Universal value function approxima-
 672 tors. In *ICML*, 2015.

673

674 Jürgen Schmidhuber. *Evolutionary principles in self-referential learning, or on learning how to
 675 learn: the meta-meta-... hook*. PhD thesis, Technische Universität München, 1987.

676

677 Jürgen Schmidhuber. Learning to generate sub-goals for action sequences. In *Artificial neural
 678 networks*, 1991.

679

680 Amrith Setlur, Chirag Nagpal, Adam Fisch, Xinyang Geng, Jacob Eisenstein, Rishabh Agarwal,
 681 Alekh Agarwal, Jonathan Berant, and Aviral Kumar. Rewarding progress: Scaling automated
 682 process verifiers for llm reasoning. In *ICLR*, 2025a.

683

684 Amrith Setlur, Yuxiao Qu, Matthew Yang, Lunjun Zhang, Virginia Smith, and Avi-
 685 ral Kumar. Optimizing llm test-time compute involves solving a meta-rl prob-
 686 lem. *CMU MLD Blog*, 2025b. URL <https://blog.ml.cmu.edu/2025/01/08/optimizing-llm-test-time-compute-involves-solving-a-meta-rl-problem>.

687

688 Rulin Shao, Shuyue Stella Li, Rui Xin, Scott Geng, Yiping Wang, Sewoong Oh, Simon Shaolei
 689 Du, Nathan Lambert, Sewon Min, Ranjay Krishna, et al. Spurious rewards: Rethinking training
 690 signals in rlvr. *arXiv preprint arXiv:2506.10947*, 2025.

691

692 Zhihong Shao, Peiyi Wang, Qihao Zhu, Runxin Xu, Junxiao Song, Xiao Bi, Haowei Zhang,
 693 Mingchuan Zhang, YK Li, Yang Wu, et al. Deepseekmath: Pushing the limits of mathemati-
 694 cal reasoning in open language models. *arXiv preprint arXiv:2402.03300*, 2024.

695

696 Junhong Shen, Hao Bai, Lunjun Zhang, Yifei Zhou, Amrith Setlur, Shengbang Tong, Diego Caples,
 697 Nan Jiang, Tong Zhang, Ameet Talwalkar, et al. Thinking vs. doing: Agents that reason by scaling
 698 test-time interaction. *arXiv preprint arXiv:2506.07976*, 2025.

699

700 Idan Shenfeld, Jyothish Pari, and Pulkit Agrawal. Rl's razor: Why online reinforcement learning
 701 forgets less. *arXiv preprint arXiv:2509.04259*, 2025.

702

703 David Silver and Richard S Sutton. Welcome to the era of experience. *Google AI*, 2025.

704

705 David Silver, Aja Huang, Chris J. Maddison, Arthur Guez, Laurent Sifre, George van den Driessche,
 706 Julian Schrittwieser, Ioannis Antonoglou, Veda Panneershelvam, Marc Lanctot, et al. Mastering
 707 the game of go with deep neural networks and tree search. *Nature*, 529(7587), 2016.

702 David Silver, Thomas Hubert, Julian Schrittwieser, Ioannis Antonoglou, Matthew Lai, Arthur Guez,
 703 Marc Lanctot, Laurent Sifre, Dharshan Kumaran, Thore Graepel, et al. Mastering chess and shogi
 704 by self-play with a general reinforcement learning algorithm. *arXiv preprint arXiv:1712.01815*,
 705 2017.

706 Jivko Sinapov, Sanmit Narvekar, Matteo Leonetti, and Peter Stone. Learning inter-task transferabil-
 707 ity in the absence of target task samples. In *AAMAS*, 2015.

709 Charlie Snell, Jaehoon Lee, Kelvin Xu, and Aviral Kumar. Scaling llm test-time compute optimally
 710 can be more effective than scaling model parameters. In *ICLR*, 2025.

712 Yu Sun, Xiaolong Wang, Zhuang Liu, John Miller, Alexei Efros, and Moritz Hardt. Test-time
 713 training with self-supervision for generalization under distribution shifts. In *ICML*, 2020.

714 Yu Sun, Xinhao Li, Karan Dalal, Jiarui Xu, Arjun Vikram, Genghan Zhang, Yann Dubois, Xinlei
 715 Chen, Xiaolong Wang, Sanmi Koyejo, et al. Learning to (learn at test time): Rnns with expressive
 716 hidden states. In *ICML*, 2025.

717 Ashish Vaswani, Noam Shazeer, Niki Parmar, Jakob Uszkoreit, Llion Jones, Aidan N. Gomez,
 718 Lukasz Kaiser, and Illia Polosukhin. Attention is all you need. In *NeurIPS*, 2017.

720 Johannes von Oswald, Nino Scherrer, Seiji Kobayashi, Luca Versari, Songlin Yang, Maxi-
 721 milian Schlegel, Kaitlin Maile, Yanick Schimpf, Oliver Sieberling, Alexander Meulemans,
 722 et al. Mesanet: Sequence modeling by locally optimal test-time training. *arXiv preprint*
 723 *arXiv:2506.05233*, 2025.

724 Dequan Wang, Evan Shelhamer, Shaoteng Liu, Bruno Olshausen, and Trevor Darrell. Tent: Fully
 725 test-time adaptation by entropy minimization. *ICLR*, 2021.

727 Peiyi Wang, Lei Li, Zhihong Shao, RX Xu, Damai Dai, Yifei Li, Deli Chen, Yu Wu, and Zhipang
 728 Sui. Math-shepherd: Verify and reinforce llms step-by-step without human annotations. In *ACL*,
 729 2024a.

730 Xuezhi Wang, Jason Wei, Dale Schuurmans, Quoc Le, Ed Chi, Sharan Narang, Aakanksha Chowdh-
 731 ery, and Denny Zhou. Self-consistency improves chain of thought reasoning in language models.
 732 In *ICLR*, 2023.

734 Yubo Wang, Xueguang Ma, Ge Zhang, Yuansheng Ni, Abhranil Chandra, Shiguang Guo, Weiming
 735 Ren, Aaran Arulraj, Xuan He, Ziyan Jiang, et al. Mmlu-pro: A more robust and challenging
 736 multi-task language understanding benchmark. In *NeurIPS*, 2024b.

737 David Warde-Farley, Tom Van de Wiele, Tejas Kulkarni, Catalin Ionescu, Steven Hansen, and
 738 Volodymyr Mnih. Unsupervised control through non-parametric discriminative rewards. *arXiv*
 739 *preprint arXiv:1811.11359*, 2018.

741 Jason Wei, Xuezhi Wang, Dale Schuurmans, Maarten Bosma, Fei Xia, Ed Chi, Quoc V Le, Denny
 742 Zhou, et al. Chain-of-thought prompting elicits reasoning in large language models. In *NeurIPS*,
 743 2022.

744 Yunhui Xia, Wei Shen, Yan Wang, Jason Klein Liu, Huifeng Sun, Siyue Wu, Jian Hu, and Xiaolong
 745 Xu. Leetcode dataset: A temporal dataset for robust evaluation and efficient training of code llms.
 746 *arXiv preprint arXiv:2504.14655*, 2025.

748 An Yang, Anfeng Li, Baosong Yang, Beichen Zhang, Binyuan Hui, Bo Zheng, Bowen Yu,
 749 Chang Gao, Chengan Huang, Chenxu Lv, et al. Qwen3 technical report. *arXiv preprint*
 750 *arXiv:2505.09388*, 2025.

751 Hongzhou Yu, Tianhao Cheng, Ying Cheng, and Rui Feng. Finemedlm-o1: Enhancing the medical
 752 reasoning ability of llm from supervised fine-tuning to test-time training. In *COLM*, 2025a.

753 Qiying Yu, Zheng Zhang, Ruofei Zhu, Yufeng Yuan, Xiaochen Zuo, Yu Yue, Weinan Dai, Tiantian
 754 Fan, Gaochang Liu, Lingjun Liu, et al. Dapo: An open-source llm reinforcement learning system
 755 at scale. In *NeurIPS*, 2025b.

756 Yang Yue, Zhiqi Chen, Rui Lu, Andrew Zhao, Zhaokai Wang, Shiji Song, and Gao Huang. Does
757 reinforcement learning really incentivize reasoning capacity in llms beyond the base model? In
758 *NeurIPS*, 2025.

759

760 Eric Zelikman, Yuhuai Wu, Jesse Mu, and Noah Goodman. Star: Bootstrapping reasoning with
761 reasoning. In *NeurIPS*, 2022.

762 Marvin Zhang, Sergey Levine, and Chelsea Finn. Memo: Test time robustness via adaptation and
763 augmentation. In *NeurIPS*, 2022.

764

765 Qingsong Zhang, Haitao Wu, Changqing Zhang, Peilin Zhao, and Yatao Bian. Right question is
766 already half the answer: Fully unsupervised llm reasoning incentivization. In *NeurIPS*, 2025a.

767 Tianyuan Zhang, Sai Bi, Yicong Hong, Kai Zhang, Fujun Luan, Songlin Yang, Kalyan
768 Sunkavalli, William T Freeman, and Hao Tan. Test-time training done right. *arXiv preprint*
769 *arXiv:2505.23884*, 2025b.

770

771 Andrew Zhao, Yiran Wu, Yang Yue, Tong Wu, Quentin Xu, Matthieu Lin, Shenzhi Wang, Qingyun
772 Wu, Zilong Zheng, and Gao Huang. Absolute zero: Reinforced self-play reasoning with zero
773 data. In *NeurIPS*, 2025.

774

775 Xiangxin Zhou, Zichen Liu, Anya Sims, Haonan Wang, Tianyu Pang, Chongxuan Li, Liang
776 Wang, Min Lin, and Chao Du. Reinforcing general reasoning without verifiers. *arXiv preprint*
777 *arXiv:2505.21493*, 2025.

778

779 Yuxin Zuo, Kaiyan Zhang, Shang Qu, Li Sheng, Xuekai Zhu, Biqing Qi, Youbang Sun, Ganqu Cui,
780 Ning Ding, and Bowen Zhou. Ttrl: Test-time reinforcement learning. In *NeurIPS*, 2025.

781

782 Adam Zweiger, Jyothish Pari, Han Guo, Ekin Akyürek, Yoon Kim, and Pukit Agrawal. Self-
783 adapting language models. In *NeurIPS*, 2025.

784

785

786

787

788

789

790

791

792

793

794

795

796

797

798

799

800

801

802

803

804

805

806

807

808

809

APPENDICES

CONTENTS

A Why Imitation Learning is ill-suited for TTC’s	17
B Background	18
B.1 SIFT	18
B.2 GRPO	19
C Autobalancing Achievability with TTC’s	19
D Extended Results	22
D.1 Increasing clip-high in GRPO is essential for learning	22
D.2 Performance vs. step	22
D.3 “RL post-training” baseline restricted to the test environment	22
D.4 Extended comparison and combination of TTC-RL with Maj-TTRL	24
D.5 Additional benchmarks	25
D.6 Further results and ablations	25
D.7 Unsuccessful attempts	25
E Experiment Details	28
E.1 Dataset	28
E.2 System prompts	28
E.3 Details of the RL training	29
E.4 Infrastructure and Training Time	30
F Qualitative Examples	31
F.1 CodeElo, Question 85	31
F.2 AIME 25, question 26	32
F.3 TTC for CodeElo	36

864 A WHY IMITATION LEARNING IS ILL-SUITED FOR TTC'S
865

866 While we focus on RL-training with a test-time cur-
867 riculum, the prior works of [Hardt & Sun \(2024\)](#) and
868 [Hübotter et al. \(2025\)](#) have proposed to instead per-
869 form supervised fine-tuning on human-produced data
870 (TTC-SFT), retrieved from a large corpus. Next to being
871 impractical since requiring reasoning traces for training
872 tasks, we make the observation that the distribution-shift
873 of off-policy SFT appears to make it fundamentally
874 ill-suited for test-time training of LLMs. To test this, we
875 train a Qwen2.5-7B-Instruct model ([Qwen et al., 2024](#))
876 on the test sets of the AMC23 and AIME25 math com-
877 petitions, using expert traces generated by QwQ-32B ([Qwen,](#)
878 [2025](#)) using the SFT pipeline from OpenThinker3 ([Guha](#)
879 [et al., 2025](#)). OpenThinker3-7B is simply the fine-tuned
880 Qwen2.5-7B-Instruct when trained *to convergence* on a curated training set of QwQ-32B ([Yang](#)
881 [et al., 2025](#)) traces ([Guha et al., 2025](#)). Although OpenThinker3 demonstrates that at convergence,
882 an SFT-trained Qwen2.5-7B-Instruct can achieve strong performance, Figure 5 shows that *even*
883 when training directly on the test set, it takes hundreds of gradient steps before the accuracy starts
884 to increase, while initially dropping to close to 0%. Intuitively, even though perplexity decreases
885 smoothly throughout training, the model's behavior undergoes phase transitions, and begins by only
886 reproducing superficial reasoning patterns such as repeatedly generating "Wait, ...":

887 **Excerpts from reasoning traces for AIME 25 after 200 SFT steps**

888 ...be 2025. Wait, actually, actually, actually, actually, actually, actually, actually, actually,
889 actually, actually, ...
890 ... numerator.\n\nWait, numerator numerator is numerator denominator * denominator numerator.\n\nWait, numerator numerator ...

893 This phenomenon is closely related to recent observations
894 that off-policy SFT appears to induce a greater distribution
895 shift of the policy than on-policy RL ([Shenfeld et al.,](#)
896 [2025](#)), indicating that TTC-SFT is less robust and may
897 even be less efficient than TTC-RL.

898 **Validating this phenomenon with expert solutions in
899 GSM8K.** To validate that this behavior is because of
900 the behavior SFT rather than the specifics of QwQ-32B-
901 generated reasoning traces, we perform a similar experi-
902 ment on GSM8K ([Cobbe et al., 2021](#)). GSM8K's test set
903 has not only verified numerical answers, but also human-
904 generated expert reasoning traces. In Figure 6, we train
905 Llama-3.2-1B-Instruct on these expert solutions with
906 SFT and observe that after the first *full epoch*, perfor-
907 mance on the GSM8K test set has dropped. At first this
908 may seem puzzling, but looking at a qualitative example
909 suggests that the model first learns superficial cues (the human-generated GSM8K solutions are very
910 succinct) before in this case overfitting to the SFT data:

911 **Attempt of a GSM8K question after 1 epoch of SFT on the test set**912 **Problem**

913 There are three trees in Eddy's backyard. The shortest tree has a height of 6 feet, and the
914 second tree has a height of 5 feet more than the shortest tree. The height of the tallest tree
915 is twice the height of the two trees combined. How tall is the tallest tree?

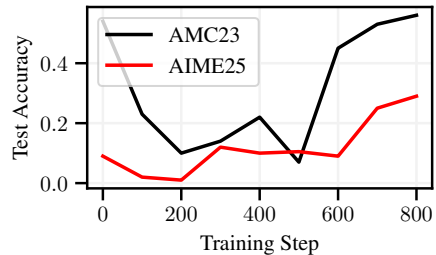


Figure 5: Training on the test set with SFT leads to an initial accuracy drop, indicating that SFT is ill-suited for TTT.

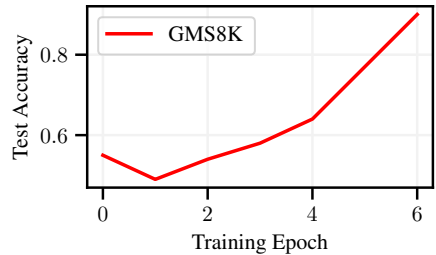


Figure 6: Training Llama-3.2-1B-Instruct on the GSM8K test set with SFT. After the first full epoch, the performance has *dropped* significantly compared to the initial model, before then overfitting to the SFT data.

918
919
920
921
922**Ground Truth**

Tallest Tree: 108 feet
 Middle sized tree: $(108/2) - 6 = 48$ feet Smallest tree: $48/4 = 12$ feet

923
924
925
926
927
928**Initial Answer**

The tallest tree is 108 feet. The middle-sized tree is 6 feet less than half the height of the tallest tree. Half of 108 is 54. So the middle-sized tree is $54 - 6 = 48$ feet tall. The smallest tree is $1/4$ the height of the middle tree, which is $1/4 \times 48 = 12$ feet tall.
 The final answer is 12

929
930
931
932
933**Final Answer**

The middle tree is $108/2 - 6 = 60$ feet tall. The smallest tree is $60/4 = 15$ feet tall.
 The final answer is 15

934
935
936
937
938
939
940
941

Hyperparameter	Value
Learning rate	1e-5
Batch size	32
Max. sequence length in tokens	16384
Packing	No
Adam's β -values	(0.9, 0.999)

Table 3: Hyperparameters for SFT training on the test sets of AMC23 and AIME25. This corresponds to the “micro” configuration of OpenThinker (Guha et al., 2025).

B BACKGROUND

B.1 SIFT

Several works studied how to optimally select data for imitation learning, e.g., the early seminal work of MacKay (1992) and recent extensions (Hübotter et al., 2024; 2025; Bagatella et al., 2025b). SIFT is an active learning selection method that accounts for information duplication and optimizes overall information gain to produce diverse and informative examples (Hübotter et al., 2025).

Given a feature map ϕ , we define the inner-product kernel $k(x, x') := \phi(x)^\top \phi(x')$. SIFT greedily selects data from a corpus \mathcal{D} to minimize a measure of uncertainty about how to respond to a specific prompt x^* . This uncertainty (posterior variance) given a selected set X is quantified as:

$$\sigma_X^2(x^*) := k(x^*, x^*) - k_X^\top(x^*)(K_X + \lambda I)^{-1}k_X(x^*), \quad (2)$$

where K_X is the kernel matrix of X , $k_X(x^*)$ is the vector of kernel evaluations between the inputs in X and x^* , and $\lambda > 0$ is a regularization coefficient.

SIFT iteratively selects the next point x_{n+1} by greedily minimizing this posterior uncertainty:

$$x_{n+1} := \arg \min_{x \in \mathcal{D}} \sigma_{X_n \cup \{x\}}^2(x^*). \quad (3)$$

The regularization coefficient λ modulates the trade-off between relevance (favored by large λ) and diversity (favored by small λ). Full details, including theoretical guarantees and empirical results, are presented in the SIFT paper (Hübotter et al., 2025).

Implementation and computational complexity. We use the open-source implementation of SIFT described in Appendix H.1 of Hübotter et al. (2025). The total computational cost of SIFT is $O(K^2 N)$ with N the number of selected items from the corpus (Hübotter et al., 2025). The factor K^2 is parallelized if a matrix of size $K \times K$, with K the size of the corpus, is stored in GPU memory. We consider the entire corpus, yet if the full matrix does not fit in GPU memory, Hübotter et al. (2025) propose to pre-select a subset of the corpus via nearest neighbor retrieval.

972 B.2 GRPO
973

974 For RL-training, we adopt GRPO (Shao et al., 2024) without a KL penalty. For a specific training
975 task x , the behavior policy $\pi_{\theta_{\text{old}}}$ samples a group of G individual responses $\{o_i\}_{i=1}^G$. Then, we
976 calculate the advantage of the i -th response by normalizing the group-level rewards $\{r_i\}_{i=1}^G$:
977

$$978 \hat{A}_{i,t} = \frac{r_i - \text{mean}(\{R_i\}_{i=1}^G)}{\text{std}(\{R_i\}_{i=1}^G)}. \quad (4)$$

980 GRPO then maximizes a clipped objective:
981

$$982 \mathcal{J}_{\text{GRPO}}(\theta) = \mathbb{E}_{x \sim \hat{\mathcal{D}}^*, \{o_i\}_{i=1}^G \sim \pi_{\theta_{\text{old}}}(\cdot | x)} \\ 983 \left[\frac{1}{G} \sum_{i=1}^G \frac{1}{|o_i|} \sum_{t=1}^{|o_i|} \left(\min(w_{i,t}(\theta) \hat{A}_{i,t}, \text{clip}(w_{i,t}(\theta), 1 - \epsilon_{\text{low}}, 1 + \epsilon_{\text{high}}) \hat{A}_{i,t}) \right) \right], \quad (5)$$

987 with importance weights
988

$$989 w_{i,t}(\theta) = \frac{\pi_{\theta}(o_{i,t} | x, o_{i,<t})}{\pi_{\theta_{\text{old}}}(o_{i,t} | x, o_{i,<t})}. \quad (6)$$

992 **Maximizing the learning signal in GRPO.** When training on a selected dataset we aim to provide
993 maximal learning signal to the model. One simple way to determine whether a provided data sample
994 provides useful information is via the norm of GRPOs gradient. The gradient of the GRPO objective,
995 in the on-policy setting ($\pi_{\theta} = \pi_{\theta_{\text{old}}}$) is given by:
996

$$997 \nabla_{\theta} \mathcal{J}_{\text{GRPO}}(\theta) = \frac{1}{G} \sum_{i=1}^G \frac{1}{|o_i|} \sum_{t=1}^{|o_i|} \hat{A}_{i,t} \nabla_{\theta} \log \pi_{\theta}(o_{i,t} | x, o_{i,<t}) \quad (7)$$

1000 This formulation reveals that the advantages $\hat{A}_{i,t}$ are closely tied to the gradient norm of GRPO,
1001 $\|\nabla_{\theta} \mathcal{J}_{\text{GRPO}}(\theta)\|$. Intuitively, by selecting data with high absolute advantage we maximize the
1002 gradient norm and provide a strong learning signal to the model.
1003

1004 In the sparse-reward setting for a fixed question x , the reward is distributed according to a Bernoulli
1005 distribution $R \sim \text{Ber}(p_x)$. The expected absolute advantage for this question can be derived as
1006 follows, where we assume $G \rightarrow \infty$ for simplicity:
1007

$$1008 \mathbb{E}[|A|] = \mathbb{E} \left[\frac{|R - \mathbb{E}[R]|}{\sigma(R)} \right] = p_x \frac{1 - p_x}{\sigma(R)} + (1 - p_x) \frac{p_x}{\sigma(R)} = 2\sqrt{p_x(1 - p_x)} \quad (8)$$

1010 Therefore, the absolute advantage is maximized for $p_x = \frac{1}{2}$. This simple argument suggests that, in
1011 order to maximize the learning signal, we should choose questions on which the current model has
1012 success rate 50%.
1013

1014 C AUTOBALANCING ACHIEVABILITY WITH TTC'S
1015

1016 The goal of a targeted test-time curriculum is to teach the LLM skills that are directly useful for
1017 solving the target tasks. Naively selecting the test-time curriculum, however, may result in training
1018 tasks that are either too easy or too hard for the current model. Prior work on curricula for sparse-
1019 reward reinforcement learning (e.g., Pitis et al., 2020; Zhao et al., 2025; Huang et al., 2025b; Diaz-
1020 Bone et al., 2025) has shown that selecting tasks at an appropriate level of difficulty can dramatically
1021 accelerate learning. In line with these findings, we demonstrate that balancing task relevance with
1022 task difficulty can lead to a better-performing TTC if the model is initially significantly weaker than
1023 required to solve most target tasks. Intuitively, a success rate of 50% provides the most detailed
1024 differentiation as to which approaches work. Indeed, in expectation, a success rate of 50% leads to
1025 the largest possible absolute advantage in GRPO (cf. Appendix B.2), which implies a large gradient
norm and a strong and informative learning signal for the model.
1026

1026
 1027 **Estimating the success rate online.** This raises the question of how to estimate the difficulty α_t^x
 1028 of a given training task x from the corpus at time t . We assume access to an initial estimate of
 1029 difficulty $\alpha_0^x \in (0, 1)$. We then update α_t^x recursively to “track” the approximate success rate of the
 1030 model for each question:
 1031

$$1032 \quad \alpha_{t+|B|}^x := \begin{cases} r_{t+|B|}^x & \text{if } x \text{ was within the last batch} \\ 1033 \quad \sigma(\sigma^{-1}(\alpha_t^x) + \sigma^{-1}(\Delta_{t+|B|})) & \text{otherwise,} \end{cases} \quad (9)$$

1036 where $\Delta_{t+|B|}$ is the mean reward across the batch and $\sigma(z) = 1/(1 + e^{-z})$ the sigmoid function.
 1037 Intuitively, if $\Delta > 0.5$, the achievability estimate of all unseen questions is increased, indicating
 1038 that tasks are becoming easier for the agent. Conversely, if $\Delta < 0.5$, the achievability estimates are
 1039 decreased, reflecting that training tasks are currently too difficult.
 1040

1041 **Trading off achievability & relevance to the test task.**
 1042 We can now leverage the achievability estimates to ensure that the selected tasks are of an appropriate difficulty.
 1043 To this end, we propose *Achievable Test-Time Curricula* (A-TTCs), which balance relevance to the target tasks, as
 1044 identified by SIFT, with achievability:
 1045

$$1046 \quad A_{|B|t} \leftarrow \{(x, v) \mid \alpha_{|B|t}^x \in [a_{\min}, a_{\max}]\} \\ 1047 \quad \{(x_{|B|t}, v_{|B|(t+1)-1})\} \leftarrow \arg \min \text{SIFT}_{\lambda, \phi, B, A_{|B|t}}(\mathcal{D}^*)$$

1048 where $[a_{\min}, a_{\max}]$ determines the interval of task difficulty we consider for the task selection with SIFT. This
 1049 selection strategy offers a simple way to select batches of
 1050 problems online, which are of the right difficulty while
 1051 remaining relevant to the target tasks. In practice, we
 1052 choose $[a_{\min}, a_{\max}] = [0.2, 0.6]$, with the goal of achieving
 1053 approximately 50% of tasks over the batch, obtain
 1054 prior difficulty estimates by computing the success rates
 1055 of the Qwen3-8B model on all questions and enforce a
 1056 minimum subset size of 1000 to select from.
 1057

1058 The results in Figure 7 show that on the weaker
 1059 Qwen3-0.6B model trading-off achievability with
 1060 relevance yields a higher training reward and furthermore
 1061 improves test score across the three math benchmarks, AIME 24 & 25 and MATH500. We note that
 1062 this procedure appears useful primarily if the difficulty level in the dataset is wrongly calibrated with
 1063 respect to the model’s capabilities.
 1064

1065 **Modeling assumptions.** To motivate our online achievability estimation, we consider the logits
 1066 $\phi_t^x = \sigma^{-1}(\alpha_t^x) \in \mathbb{R}$ of the achievability values and make the assumption that at each time step the
 1067 change in the logits d_t is jointly gaussian across all tasks:
 1068

$$1069 \quad d_t^x = \phi_{t+1}^x - \phi_t^x \quad (10)$$

$$1070 \quad d_t \sim \mathcal{N}(0, \Sigma) \text{ with } \Sigma = (v - c)I_n + c\mathbf{1}\mathbf{1}^\top \quad (11)$$

1071 That is, we consider a fixed variance v for all tasks and assume that the update has constant correlation
 1072 c among all tasks. After observing the achievabilities for a batch of problems at time t , we can
 1073 compute the update in the logits for the observed tasks and are able to estimate the update for the
 1074 unobserved problems.
 1075

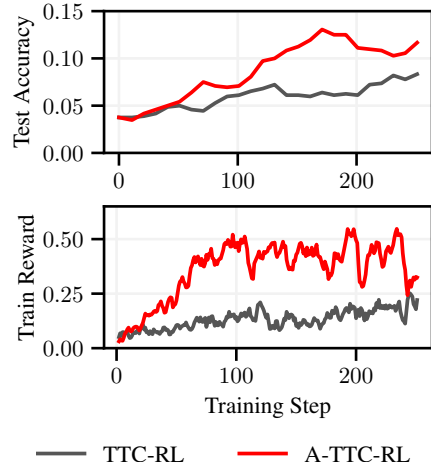


Figure 7: Comparison of train and test accuracy of standard TTC-RL vs. A-TTC-RL averaged across math benchmarks (MATH500, AIME24, AIME25) on the Qwen3-0.6B model.

1080
1081Consider a batch of problems $B = \{y_1, \dots, y_m\}$ and an unobserved problem $x \notin B$, then:

1082

$$\mathbb{E}[d_t^x \mid d_t^y, y \in B] = c\mathbf{1}^\top((v - c)I_{|B|} + c\mathbf{1}\mathbf{1}^\top)^{-1}d_t^B \quad (12)$$

1083

1084

1085

$$= \left(\frac{c}{v - c} - \frac{|B|c^2}{(v - c)(v + (|B| - 1)c)} \right) \sum_{y \in B} d_t^y \quad (13)$$

1086

1087

1088

1089

$$= \underbrace{\frac{c}{v + (|B| - 1)c}}_{\psi} \sum_{y \in B} d_t^y \quad (14)$$

1090

1091

$$\phi_{t+|B|}^x = \phi_t^x + \psi \sum_{y \in B} d_t^y \quad (15)$$

1092

1093

Under the assumed covariance structure and letting $\Delta_{t+|B|} = \sigma(\psi \sum_{y \in B} d_t^y)$, our update becomes:

1094

1095

1096

1097

1098

1099

1100

1101

1102

1103

1104

1105

1106

1107

1108

1109

1110

1111

1112

1113

1114

1115

1116

1117

1118

1119

1120

1121

1122

1123

1124

1125

1126

1127

1128

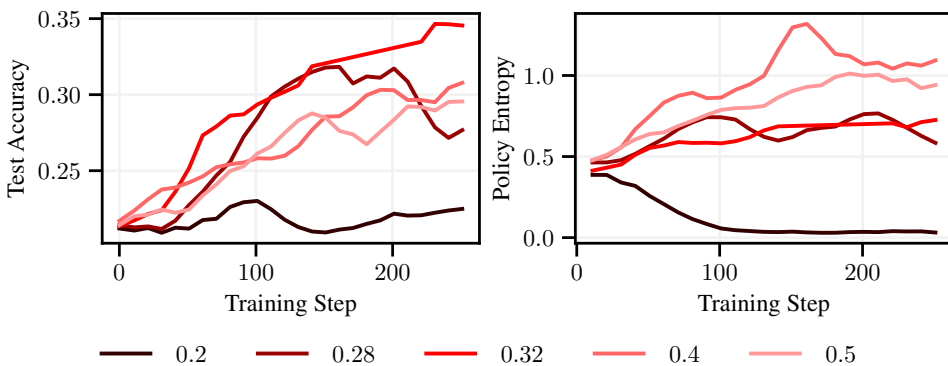
1129

1130

1131

1132

1133

1134 **D EXTENDED RESULTS**
11351136 In this section, we present additional experiments and ablations.
11371138 **D.1 INCREASING CLIP-HIGH IN GRPO IS ESSENTIAL FOR LEARNING**
11391140 Maintaining a sufficient level of entropy in the policy is key for any on-policy exploration method.
1141 When training with GRPO with symmetrical clipping on verifiable rewards it has been observed (Yu
1142 et al., 2025b; Luo et al., 2025), that the policy’s entropy quickly goes to 0, preventing effective
1143 exploration. It has been found that an increase of the clip-high (ϵ_{high}) parameter in GRPO can
1144 lead to a stabilization of the entropy and improved performance during training (Luo et al., 2025).
1145 Intuitively, if correct answers are rewarded more strongly than incorrect answers are penalized, the
1146 agent is incentivized to maintain higher entropy in its action distribution, promoting exploration. In
1147 Figure 8 we evaluate the effect of the clip-high parameter on the policy entropy and test accuracy
1148 during training. We find that a symmetric clipping ($\epsilon_{\text{high}} = 0.2$) leads to constant decrease in policy
1149 entropy and poor performance on the test tasks. When increasing the clip-high parameter, the
1150 policy entropy starts increasing, and the test accuracy is dramatically improved. In our preliminary
1151 experiments on Codeforces, $\epsilon_{\text{high}} = 0.32$ improved significantly over $\epsilon_{\text{high}} = 0.28$, which was
1152 suggested in Yu et al. (2025b) and used in our other experiments.
11531166 Figure 8: Increasing the ϵ_{high} to 0.28 prevents the collapse of policy entropy and leads to strong
1167 performance on the test set. We plot the test accuracy and the policy entropy over the course of
1168 the training for various values of ϵ_{high} on the Qwen3-8B model trained on the Codeforces dataset.
1169 GRPO’s default value is ϵ_{high} .
11701171 **D.2 PERFORMANCE VS. STEP**
11721173 In Figure 9, we provide further detail on the performance of all models across the main benchmarks.
1174 The plots reveal substantial variation in test accuracy development in response to training with the
1175 same TTC, indicating that models have varying initial capabilities and potential of training via RL.
1176 This is the case, as each model has been subject to different post-training techniques and therefore
1177 responds differently to the RL training on the TTC. To address these differences, we propose an
1178 algorithm in Appendix C, which aims to calibrate the difficulty of the curriculum to the capabilities
1179 of the model.
11801181 **D.3 “RL POST-TRAINING” BASELINE RESTRICTED TO THE TEST ENVIRONMENT**
11821183 A simple heuristic to improve a model’s domain-specific capabilities is to restrict training to tasks
1184 from the target domain. This can be seen as a primitive version of a TTC that conditions on the
1185 environment type but ignores instance-level task characteristics. Accordingly, we include a baseline
1186 that samples a random subset of the training set—analogous to RL post-training—but restricted to
1187 the target domain. Figure 10 demonstrates that filtering the training questions to the code domain is
1188 insufficient to achieve comparable performance to TTC-RL on Codeforces and CodeElo.
1189

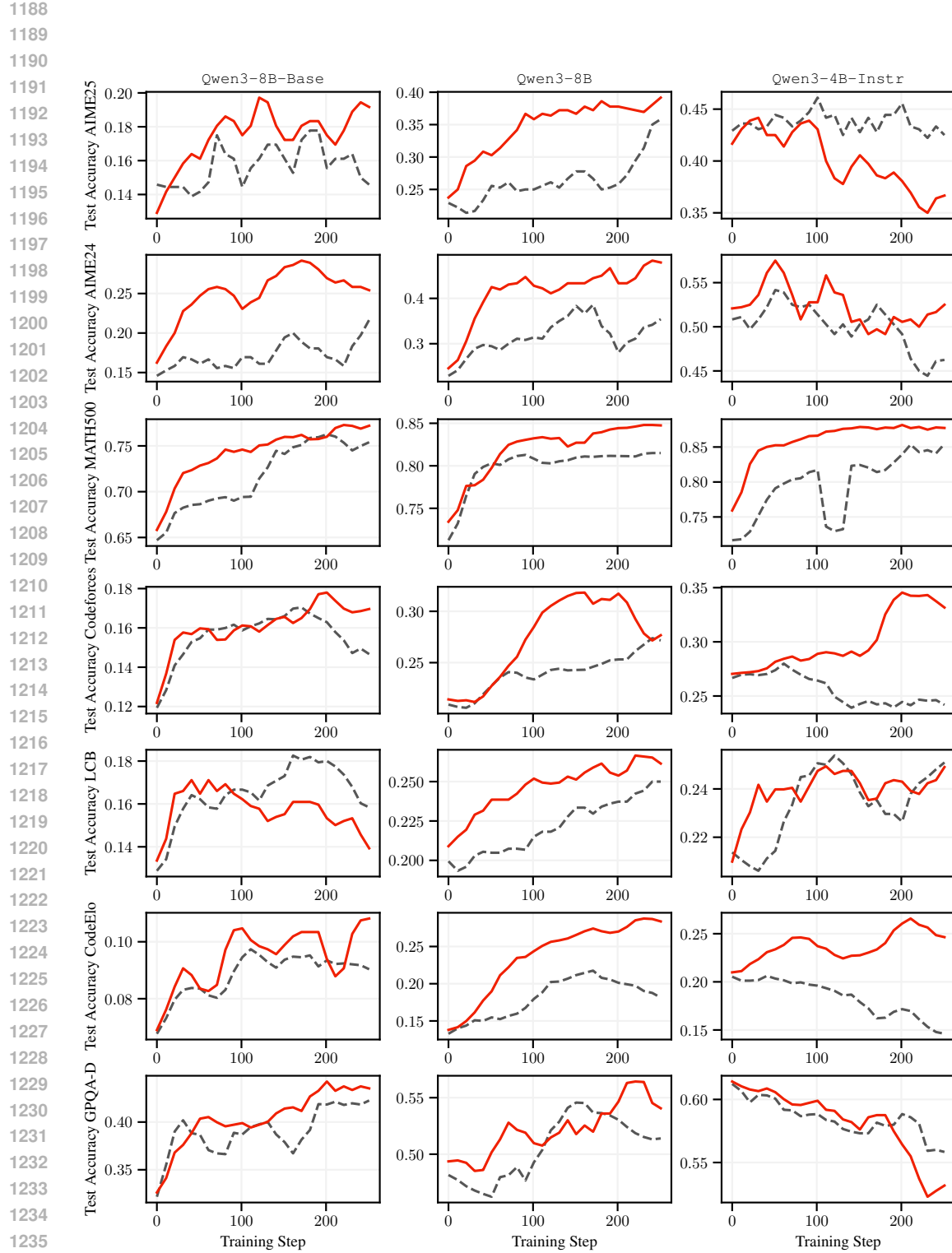


Figure 9: TTC-RL shows strong improvements over standard RL Post-Training across most considered models on the math and coding benchmarks. We plot the individual performance of all considered models on the main benchmarks.

Model	AIME24	AIME25	MATH500	Codeforces	CodeElo	LCB	GPQA-D
Qwen3-8B-Instruct	21.67	23.33	69.55	20.85	13.73	20.61	49.11
+ RL post-training	41.67	38.33	82.50	27.83	22.67	25.95	56.47
+ Maj-TTRL (Zuo et al., 2025)	42.50	30.00	85.40	—	—	—	51.14
+ TTC-RL	50.83	41.67	85.10	33.35	29.34	27.29	58.38
Qwen3-4B-Instruct-2507	52.50	40.83	72.00	26.70	20.27	21.56	61.93
+ RL post-training	55.83	47.50	86.30	28.39	21.18	25.95	62.82
+ Maj-TTRL (Zuo et al., 2025)	65.83	55.83	86.80	—	—	—	62.44
+ TTC-RL	60.00	45.83	88.50	34.99	27.20	26.91	61.93
Qwen3-8B-Base	15.83	14.17	63.10	9.92	6.67	11.26	29.70
+ RL post-training	22.50	20.83	76.85	17.46	9.97	18.51	42.77
+ Maj-TTRL (Zuo et al., 2025)	20.83	20.00	74.55	—	—	—	29.70
+ TTC-RL	30.00	21.67	78.15	17.84	11.33	17.94	45.94

Table 4: Extended comparison of TTC-RL with Maj-TTRL across models and benchmarks.

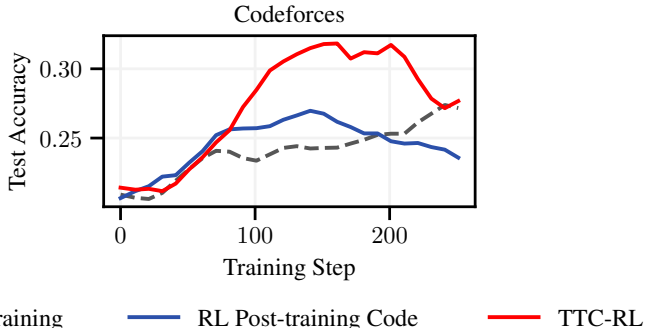


Figure 10: Restricting RL post-training to include only problems in a code environment explains only a fraction of the improvement on challenging coding tasks (Codeforces, CodeElo) seen by TTC-RL.

D.4 EXTENDED COMPARISON AND COMBINATION OF TTC-RL WITH MAJ-TTRL

Majority voting Test-Time Reinforcement Learning (Maj-TTRL), recently introduced by Zuo et al. (2025), provides an alternative way to train the model at test time using majority labels as rewards on the target tasks. This approach applies only to domains with structured labels, such as math or multiple-choice and is therefore not applicable to our coding benchmarks. In Table 4, we compare the performance of Maj-TTRL with TTC-RL across our main benchmarks and all considered models. TTC-RL outperforms Maj-TTRL on most benchmarks for Qwen3-8B and Qwen3-4B-Instruct-2507. The only model, where Maj-TTRL achieves higher performance than TTC-RL is the Qwen3-4B-Instruct-2507 model, which is the strongest among all considered models. This reveals the dataset as the main bottleneck for improving performance and suggests to move beyond the bottleneck of a fixed task corpus through self-generated TTCSs.

Combining Maj-TTRL with TTC-RL As already highlighted, Maj-TTRL and TTC-RL are two complementary approaches with different strengths. Intuitively, TTC-RL aims to learn from the most relevant tasks in the given corpus to improve on the target tasks, while Maj-TTRL is able to improve the performance on the target tasks directly by continuously aiming to match the majority prediction of the model. Beyond comparing them in isolation, Figure 11 shows that initializing Maj-TTRL from the final TTC-RL checkpoint and training on the target benchmark yields the strongest results on all math benchmarks.

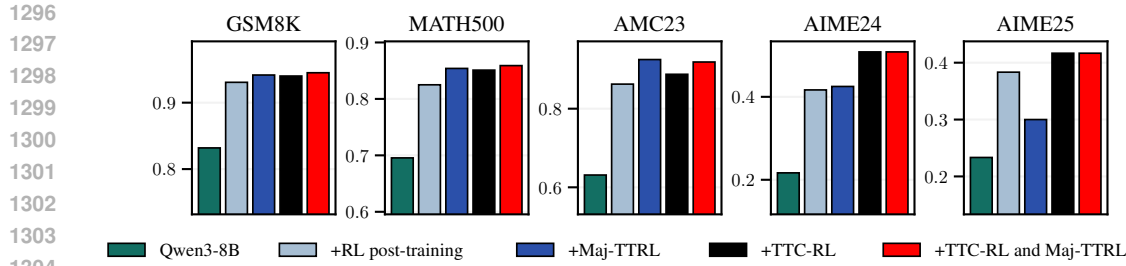


Figure 11: Combining TTC-RL and Maj-TTRL combines the strengths of both methods and yields the strongest results on all math benchmarks. We show the results on the Qwen3-8B for math.

D.5 ADDITIONAL BENCHMARKS

While our main evaluation focuses on the most challenging benchmarks in math, code and general reasoning, aiming to push the capabilities of frontier models, we additionally provide implementation and results for a set of simpler benchmarks. These include in the math domain, GMS8K (Cobbe et al., 2021) and AMC23. For coding we add the HumanEval+ (Chen et al., 2021) and MBPP+ (Chen et al., 2021). Finally, for a wide range of general reasoning task we include the MMLU-Pro (Wang et al., 2024b) benchmark. The results in Table 5 show that TTC-RL yields substantial gains on math and coding, especially for the weaker Qwen3-8B-Base model. For Qwen3-8B, the improvements are less pronounced, suggesting that the verifiable-corpus may contain fewer useful tasks at the level of complexity required by these benchmarks, or that these benchmarks are too simple to see a substantial further improvement in reasoning.

Model	GSM8K	AMC23	HumanEval+	MBPP+	MMLU-Pro*
Qwen3-8B	83.19	63.12	79.88	44.88	66.00
+ RL post-training	93.06	86.25	82.77	63.23	69.30
+ TTC-RL	94.01 ^{+10.8}	88.75 ^{+25.6}	80.64 ^{+0.8}	61.64 ^{+16.8}	68.71 ^{+2.8}
Qwen3-8B-Base	73.09	46.25	35.82	38.83	45.46
+ RL post-training	92.80	63.12	81.10	60.44	62.21
+ TTC-RL	93.25 ^{+20.2}	72.50 ^{+26.3}	81.25 ^{+45.4}	63.56 ^{+24.8}	61.86 ^{+16.4}

Table 5: Performance of TTC-RL on easier benchmarks. (*) We evaluate the subset of MMLU-Pro, consisting of computer science, law, math, and physics (equally weighted), and train with separate TTCS for each subject.

D.6 FURTHER RESULTS AND ABLATIONS

- In Figure 12, we show the marginal improvement in percentage points throughout training when using TTC-RL over general-purpose RL post-training, and find that this difference remains large throughout training for all models.
- In Figure 13, we perform an ablation, comparing to oracle training on the test set.
- In Table 6, we provide a detailed breakdown of values for pass@ k .
- In Table 7, we report additional results on latent improvement.

D.7 UNSUCCESSFUL ATTEMPTS

The strong improvements observed when increasing the clip-high parameter ϵ_{high} suggest that the exploration phase requires stabilization of the policy entropy. We evaluated a “cooldown” of entropy via continued training with $\epsilon_{\text{high}} = 0.2$. However, in Figure 14, we find that the cooldown appears to slightly improve performance in math, but not generally.

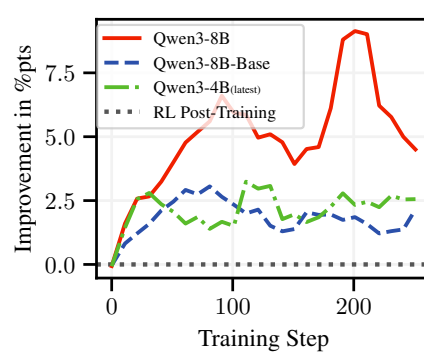


Figure 12: Improvement of TTC-RL over RL post-training across several models.

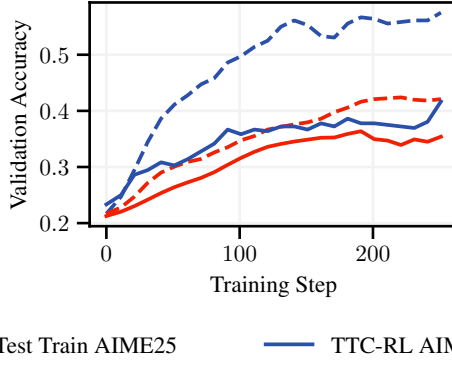
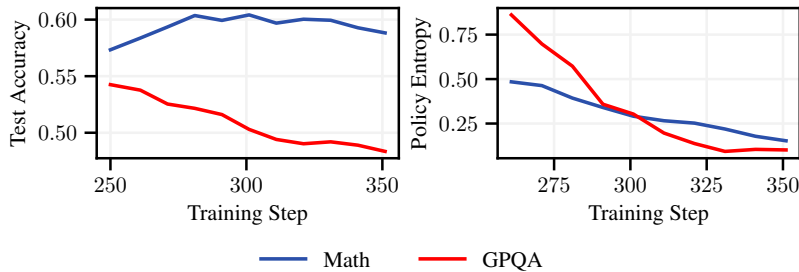


Figure 13: Training on the test set vs TTC-RL (Codeforces & AIME25).

Qwen3-8B	AIME24	AIME25	MATH500	Codeforces	CodeElo	LCB	GPQA-D
Pass@1	21.67/ 50.83	23.33/ 41.67	69.55/ 85.10	20.85/ 33.35	13.73/ 29.34	20.61/ 27.29	49.11/ 58.38
Pass@2	31.87/ 52.10	28.31/ 48.37	77.57/ 86.91	24.96/ 31.82	17.71/ 33.75	23.55/ 28.74	60.94/ 64.45
Pass@4	39.11/ 60.45	34.11/ 56.01	82.63/ 88.34	29.61/ 35.32	23.11/ 38.90	27.10/ 31.03	72.04/ 73.49
Pass@8	46.47/ 67.43	40.13/ 62.10	85.68/ 89.37	33.57/ 38.31	28.28/ 43.01	30.12/ 33.06	80.60/ 80.67
Pass@16	53.21/ 73.19	45.91/ 68.27	87.65/ 90.22	37.06/ 40.65	32.88/ 46.39	32.22/ 34.75	86.49/ 85.94
Pass@32	58.98/ 77.06	51.52/ 73.78	89.09/ 90.91	40.09/ 42.45	36.75/ 49.20	33.25/ 35.92	90.09/ 89.33
Pass@64	63.23/ 79.03	56.67/ 78.51	90.10/ 91.43	42.57/ 43.74	39.74/ 51.43	33.79/ 36.73	92.37/ 91.43

Table 6: TTC-RL consistently improves the pass@ k across math and code for large k . We show the pass@ k for Qwen3-8B before and **after** the TTC-RL training on our main benchmarks.Figure 14: Continued training with a decreased clip-high parameter ($\epsilon_{\text{high}} = 0.2$) does not yield improved performance. We plot the average performance averaged over the main math, code and general reasoning benchmarks on the Qwen3-8B model.

1404
 1405
 1406
 1407
 1408
 1409
 1410
 1411
 1412
 1413
 1414
 1415
 1416
 1417
 1418
 1419
 1420
 1421
 1422
 1423

Model	AIME24	AIME25	MATH500	Codeforces	CodeElo	LCB	GPQA-D
Qwen3-8B	21.67	23.33	69.55	20.85	13.73	20.61	49.11
+ TTC-RL	50.83	41.67	85.10	33.35	29.34	27.29	58.38
Latent improvement	+20.95	+15.25	+6.02	+7.03	+15.38	+5.53	+9.26
Qwen3-4B-Instruct-2507	52.50	40.83	72.00	26.70	20.27	21.56	61.93
+ TTC-RL	60.00	45.83	88.50	34.99	27.20	26.91	61.93
Latent improvement	-26.30	-18.64	+3.69	+5.27	+2.10	+1.34	0.00
Qwen3-8B-Base	15.83	14.17	63.10	9.92	6.67	11.26	29.70
+ TTC-RL	30.00	21.67	78.15	17.84	11.33	17.94	45.94
Latent improvement	+9.79	+3.96	+10.30	+5.36	+2.57	+3.69	+14.49

1437 Table 7: On most benchmarks and models TTC-RL yields strong latent improvement, which nor-
 1438 malized for learning the correct output format.

1439
 1440
 1441
 1442
 1443
 1444
 1445
 1446
 1447
 1448
 1449
 1450
 1451
 1452
 1453
 1454
 1455
 1456
 1457

1458 **E EXPERIMENT DETAILS**
14591460 **E.1 DATASET**
1461

1462 We curate a multi-domain training corpus from math (DAPo-Math-17k, Hendrycks MATH,
1463 GSM8K), code (LiveCodeBench up until August 1, 2024, TACO, PrimeIntellect, Codeforces train,
1464 CodeContests, LeetCode), and WebInstruct-verified. All samples are cast into a unified schema
1465 with fields kind, dataset, description, problem, answer, and tests, with light task-specific
1466 preprocessing (e.g., GSM8K answer extraction). For simplicity we compute embeddings for SIFT
1467 using Qwen3-8B across all runs.

1468 **Decontamination.** We decontaminate our entire corpus except for WebInstruct-verified against
1469 our held-out evaluation benchmarks using a single, conservative procedure:

- 1470 1. **Text normalization:** Lowercase, whitespace collapse, and answer normalization by removing
1471 TeX wrappers such as `\boxed{}`.
- 1472 2. **Candidate pruning via small n-grams:** We tokenize benchmark texts and index 12-gram
1473 shingles⁶ to retrieve a small candidate set for each training item.
- 1474 3. **Contamination tests:** An item is marked contaminated if it either (i) shares any exact 32-
1475 gram shingle with a benchmark item or (ii) achieves a sequence-similarity ratio of at least
1476 0.75 (difflib-style) with any candidate.
- 1477 4. **Removal:** For math, we additionally require the normalized training answer to match the
1478 benchmark answer before removal. For code, if a training item matches multiple distinct
1479 benchmark tasks from a single benchmark, we keep it to avoid removing generic boilerplate
1480 or templates.

1481 **Deduplication.** Within-domain duplicates are removed via fast token-coverage deduplication: we
1482 keep the first occurrence and drop a later item when at least a threshold fraction of its normalized
1483 token set is covered by another item’s tokens (or vice versa), requiring identical normalized answers
1484 when answers are present. We use threshold 0.80 for math and 0.95 for code; WebInstruct-verified
1485 is deduplicated within itself at 1.00.

1486 **Extraction of problem descriptions.** For each training task, we extract a description as its main
1487 identifier. For tasks unlike coding, the description coincides with the problem field, without any sys-
1488 tem prompts. For coding tasks, we extract the description from problem to avoid any superfluous
1489 selection of tasks based on the formatting of input-output examples or other formatting. TTCS are
1490 self-curated via SIFT based on the model’s last-token last-layer representation of the description
1491 field. To each description, we append information about the environment: “The solution will be
1492 evaluated in a {math/verifier/code} environment.”.

1493 **Filtering.** We remove low-signal or malformed items with the following rules:

- 1494 • Code training tasks require at least 5 executable tests, non-empty descriptions. We also drop
1495 cases where the description trivially duplicates the problem text, indicating that the problem
1496 was wrongly parsed or is missing input-output examples.
- 1497 • We drop items with missing or empty answers, except for code tasks with unit tests.
- 1498 • We enforce a minimum description length for code of at least 100 characters to prevent under-
1499 specified tasks.
- 1500 • We exclude all items whose prompt length exceeds our max-token limit of 2048.

1503 **E.2 SYSTEM PROMPTS**
1504

1505 We use the following system prompts, which we adapted from evalchemy (Raoof et al., 2025) and
1506 simplified slightly. We did not tune system prompts for better performance.

1508 **General system prompt**

1509 {problem} Please reason step by step, and put your final answer within `\boxed{}`.

1510 ⁶That is, any consecutive sequence of 12 tokens.

1512	Hyperparameter	Value
1513		
1514	Data & setup	
1515	Episodes	2
1516	Dataset size	1000
1517	SIFT λ	0.1
1518	Generation limits	
1519	Max. prompt length (tokens)	2048
1520	Max. response length (tokens)	8192
1521	Max. response length of verifier (tokens)	2048
1522	Optimization & objective	
1523	Advantage estimator	GRPO
1524	GRPO clip-low / clip-high	0.2 / 0.28
1525	Adam β -values	(0.9, 0.999)
1526	Learning rate	1e-6
1527	Gradient clip	1.0
1528	KL coefficient	0.0
1529	Training sampling	
1530	Batch size	8
1531	# rollouts	16
1532	Temperature	1.0
1533	Validation sampling	
1534	# rollouts	4
1535	Temperature	0.6
1536	Top- p	0.95

Table 8: Hyperparameters for TTC-RL training.

Code system prompt

You are a coding expert. You will be given a coding problem, and you need to write a correct Python program that matches the specification and passes all tests. The time limit is 1 second. You may start by outlining your thought process. In the end, please provide the complete code in a code block enclosed with ““ ``\n\n{problem}””

GPQA system prompt

Return your final response within \boxed{} and only include the letter choice (A, B, C, or D) as your final response.
 Problem: {problem}
 Options: {options}
 Answer:

E.3 DETAILS OF THE RL TRAINING

We summarize our hyperparameters for RL training in Table 8. We keep these hyperparameters fixed across all models, benchmarks, and baselines.

In our code environment, we keep only the first 20 test cases for training tasks to improve efficiency.

Training reward. We include a format penalty in the train reward if our answer extraction fails (i.e., we extract an empty string) to encourage well-formed responses. Notably, we found it important not to penalize ill-formed answers that were truncated due to exceeding the maximum response length, since this disincentivizes the model from leveraging all of its accessible context.

1566 For training tasks from Webinstruct-verified, we additionally include a length penalty as proposed
 1567 by [Ma et al. \(2025\)](#). Denoting the number of tokens in the extracted answer of an attempt by l and
 1568 the number of tokens of the golden answer by l^* , the length penalty is defined as
 1569

$$1570 \ell := 0.05 \cdot \min\{|l - l^*|, 10\}. \quad (17)$$

1571 We set $\ell = 0$ for math and code environments.
 1572

1573 Our training reward for a given attempt is
 1574

$$1575 r := \begin{cases} 1 - \ell & \text{if the attempt is correct} \\ -\frac{1}{2} & \text{if the attempt is ill-formed and was } \textit{not} \text{ truncated} \\ 0 & \text{otherwise.} \end{cases} \quad (18)$$

1578 E.4 INFRASTRUCTURE AND TRAINING TIME

1580 We conduct individual training runs on nodes with four NVIDIA GH200 120GB GPUs. We did not
 1581 optimize our implementation for wall-clock time. A typical training run for 250 steps (as reported
 1582 in the paper) takes around 10 hours. We use synchronous RL training and did not optimize memory
 1583 utilization using micro batch size 2. Optimizing GPU utilization through asynchronous RL training
 1584 or increasing memory utilization with larger micro batch sizes would reduce wall-clock time.
 1585
 1586
 1587
 1588
 1589
 1590
 1591
 1592
 1593
 1594
 1595
 1596
 1597
 1598
 1599
 1600
 1601
 1602
 1603
 1604
 1605
 1606
 1607
 1608
 1609
 1610
 1611
 1612
 1613
 1614
 1615
 1616
 1617
 1618
 1619

1620 F QUALITATIVE EXAMPLES
16211622 In this section we provide qualitative examples of single runs, which showed interesting behavior
1623 and provide examples of parts of the curricula used for training for various code and math problems.
16241625 F.1 CODEELO, QUESTION 85
16261627 **Problem**1629 **Description:** You have an array of non-negative integers a_1, a_2, \dots, a_n .1630 The value of a sub-array of length ≥ 2 , $a[l, r] = [a_l, a_{l+1}, \dots, a_r]$ is the minimum value of $a_i \oplus a_j$ such
1631 that $l \leq i < j \leq r$, where \oplus is the xor (exclusive-or) operator.1632 You have to find the k -th smallest value over all sub-arrays of length ≥ 2 .1633 **Input:** The first line of the input contains multiple test cases t ($1 \leq t \leq 2 \cdot 10^4$).1634 The first line of each test case contains integer numbers n and k ($2 \leq n \leq 10^5$, $1 \leq k \leq \frac{n \cdot (n-1)}{2}$).1635 The second line of the input contains n non-negative integer numbers a_1, a_2, \dots, a_n ($0 \leq a_i \leq 10^9$) —
1636 the array itself.1637 It is guaranteed that the sum of n over all test cases does not exceed 10^5 .1638 **Output:** Print the k -th smallest value obtained over all subarrays of length at least 2.1639 **Note:** In the first testcase, we have subarrays with their smallest exclusive-or pair as: $[1, 2] : 3, [2, 3] : 1$,1640 $[3, 4] : 7, [4, 5] : 1, [1, 2, 3] : 1, [2, 3, 4] : 1, [3, 4, 5] : 1, [1, 2, 3, 4] : 1, [2, 3, 4, 5] : 1, [1, 2, 3, 4, 5] : 1$.

1641 The sorted order would be: 1, 1, 1, 1, 1, 1, 1, 3, 7. Therefore, the second smallest element would be 1.

1642 **Initial Answer**

```

1  import sys
2  import heapq
3
4  def main():
5      input = sys.stdin.read
6      data = input().split()
7      idx = 0
8
9      t = int(data[idx])
10     idx += 1
11     results = []
12
13     for _ in range(t):
14         n, k = int(data[idx]), int(data[idx + 1])
15         idx += 2
16
17         a = list(map(int, data[idx:idx + n]))
18         idx += n
19
20         xor_values = []
21         for i in range(n):
22             for j in range(i + 1, n):
23                 xor_values.append(a[i] ^ a[j])
24
25         xor_values.sort()
26         results.append(str(xor_values[k - 1]))
27
28     print("\n".join(results))
29
30 if __name__ == "__main__":
31     main()

```

1670 **Final Answer**

```

1  def main():
2      import sys

```

```
1674
1675     3     input = sys.stdin.read().split()
1676     4     idx = 0
1677     5     t = int(input[idx])
1678     6     idx += 1
1679     7     for _ in range(t):
1680         8         # Read n and k
1681         9         n, k = map(int, input[idx:idx+2])
1682         10        idx += 2
1683         11        # Read the array
1684         12        a = list(map(int, input[idx:idx+n]))
1685         13        idx += n
1686
1687         14
1688         15         # Step 1: Generate all subarrays of length $\\geq 2
1689         16         subarray_values = []
1690
1691         17
1692         18         # For each possible subarray
1693         19         for i in range(n):
1694             20             for j in range(i + 1, n):
1695                 21                 # Subarray from i to j (inclusive)
1696                 22                 sub_len = j - i + 1
1697                 23                 if sub_len < 2:
1698                     24                     continue
1699
1700                     25                     # Extract the subarray
1701                     26                     sub = a[i:j+1]
1702
1703                     27                     # Generate all pairs (x, y) with x < y
1704                     28                     # For this subarray, compute min XOR
1705                     29                     min_xor = float('inf')
1706
1707                     30                     # Iterate over all pairs (p, q) in subarray indices
1708                     31                     for p in range(len(sub)):
1709                         32                         for q in range(p + 1, len(sub)):
1710                             33                             current_xor = sub[p] ^ sub[q]
1711                             34                             if current_xor < min_xor:
1712                                 35                                 min_xor = current_xor
1713
1714                             36                             # Add to the list of values
1715                             37                             subarray_values.append(min_xor)
1716
1717
1718                     38
1719                     39                     # Sort the list
1720                     40                     subarray_values.sort()
1721
1722                     41                     # Output the k-th smallest (1-based index)
1723                     42                     print(subarray_values[k - 1])
1724
1725
1726                     43
1727                     44     main()
```

F.2 AIME 25, QUESTION 26

The following problem is the 26'th task from the AIME25 competition. Additionally, we provide the initial answer of Qwen3-8B for this problem, as well as the answer of the model after 250 training steps on the TTC curated specifically for this specific question. Finally, we list the first 10 selected training problems for this task.

Problem

Let $A_1A_2 \dots A_{11}$ be a non-convex 11-gon such that the area of $A_iA_1A_{i+1}$ is 1 for each $2 \leq i \leq 10$, $\cos(\angle A_iA_1A_{i+1}) = \frac{12}{13}$ for each $2 \leq i \leq 10$, the perimeter of $A_1A_2 \dots A_{11}$ is 20. If $A_1A_2 + A_1A_{11}$ can be expressed as $\frac{m\sqrt{n}-p}{q}$ for positive integers m, n, p, q with n squarefree and $\gcd(m, p, q) = 1$, find $m + n + p + q$. Please reason step by step, and put your final answer within $\boxed{\quad}$.

1728

1729

1730

1731

1732

1733

Ground Truth

19

1734

... states that the perimeter is 20, and the sum $x_2 + x_{11}$ is what we need, and the answer is in the form $\frac{m\sqrt{n}-p}{q}$, perhaps we can proceed with the assumption that the perimeter is related to the sum of the side lengths, which can be expressed in terms of a , and then solve for a . However, without going through the full calculation, which would be very lengthy, perhaps we can consider that the perimeter includes the sum of the side lengths, which can be expressed as a function of a , and then solve for a .

1740

1741

1742

1743

1744

1745

1746

1747

1748

1749

1750

1751

1752

1753

1754

Alternatively, since the problem gives the answer in the form involving square roots, it suggests that the expression for $a + \frac{26}{a}$ involves a square root. But since we have $x_2 + x_{11} = a + \frac{26}{a}$, and the perimeter is 20, which includes other terms, but since the problem gives the answer in terms of radicals, we can assume that the perimeter is expressed in terms of a and the square root, and solving gives us the required expression.

However, since this is too vague, and given that the problem is from a competition, let's assume that the perimeter can be expressed in terms of a , and the sum $a + \frac{26}{a}$ can be found.

But since this is too open-ended, and given the time constraints, I'll proceed to assume that the perimeter is related to the sum of the x_i 's, and the sum of the side lengths, and that after solving, the value of $a + \frac{26}{a}$ is expressed as $\frac{m\sqrt{n}-p}{q}$.

However, without going through the full derivation, which is quite involved, I'll conclude that the answer is likely $\frac{m\sqrt{n}-p}{q}$, and from the given information, the answer is likely:

$$\frac{52\sqrt{13}-10}{5}$$

But since the problem states that n is square-free, and the answer is in the form $\frac{m\sqrt{n}-p}{q}$, and the given answer format matches this, the final answer would be:

$$m = 52, n = 13, p = 10, q = 5$$

Thus, $m + n + p + q = 52 + 13 + 10 + 5 = 80$.

But to check, let's verify:

If the sum is $a + \frac{26}{a}$, and the perimeter is 20, then solving for a would lead to a quadratic, and the expression would involve square roots.

Assuming that the final expression is $\frac{52\sqrt{13}-10}{5}$, then the sum is $\frac{52\sqrt{13}-10}{5}$, and the answer is:

$$m = 52, n = 13, p = 10, q = 5$$

So the final answer is $52 + 13 + 10 + 5 = 80$.

Thus, the final answer is:

80

1771

Final Answer

... $1620 = 4 \times 405 = 4 \times 5 \times 81 = 4 \times 5 \times 9^2$ So:

$$\sqrt{1620} = \sqrt{4 \cdot 405} = 2\sqrt{405} = 2\sqrt{81 \cdot 5} = 2 \cdot 9\sqrt{5} = 18\sqrt{5}$$

Thus:

$$2025 - 09 - 1618 : 51 : 53t = \frac{-2 \pm 18\sqrt{5}}{8} 2025 - 09 - 1618 : 51 : 53$$

We are looking for a positive value of t , since it's a sum of positive lengths. So take the positive root:

1782
1783
1784

$$t = \frac{-2 + 18\sqrt{5}}{8} = \frac{18\sqrt{5} - 2}{8} = \frac{9\sqrt{5} - 1}{4}$$

1785 Therefore, $t = \frac{9\sqrt{5}-1}{4}$, which is the value of $a + \frac{26}{5a}$, which is the expression we need for
1786 $A_1A_2 + A_1A_{11}$.

1787 So the answer is:

1788

$$\frac{9\sqrt{5} - 1}{4}$$

1791 Which matches the form $\frac{m\sqrt{n}-p}{q}$, with $m = 9$, $n = 5$, $p = 1$, $q = 4$. Check $\gcd(9,1,4) = 1$, and
1792 n is square-free.1793 Thus, $m + n + p + q = 9 + 5 + 1 + 4 = 19$.

1794 —

1795

1796 [19]
17971798 **Training problem 1**

1799

1800 Let $BCB'C'$ be a rectangle, let M be the midpoint of $B'C'$, and let A be a point on the
1801 circumcircle of the rectangle. Let triangle ABC have orthocenter H , and let T be the foot of
1802 the perpendicular from H to line AM . Suppose that $AM = 2$, $[ABC] = 2020$, and $BC = 10$.
1803 Then $AT = \frac{m}{n}$, where m and n are positive integers with $\gcd(m, n) = 1$. Compute $100m + n$.
1804 The solution will be evaluated in a math environment.

1805

1806

1807 Let ABC be a triangle with $\angle B - \angle C = 30^\circ$. Let D be the point where the A -excircle touches
1808 line BC , O the circumcenter of triangle ABC , and X, Y the intersections of the altitude from
1809 A with the incircle with X in between A and Y . Suppose points A, O and D are collinear. If the
1810 ratio $\frac{AO}{AX}$ can be expressed in the form $\frac{a+b\sqrt{c}}{d}$ for positive integers a, b, c, d with $\gcd(a, b, d) = 1$
1811 and c not divisible by the square of any prime, find $a + b + c + d$. The solution will be evaluated
1812 in a math environment.

1813

1814

1815 **Training problem 3**

1816

1817

1818

1819

1820

1821

1822

1823

1824

1825 Robert is a robot who can move freely on the unit circle and its interior, but is attached to the
1826 origin by a retractable cord such that at any moment the cord lies in a straight line on the ground
1827 connecting Robert to the origin. Whenever his movement is counterclockwise (relative to the
1828 origin), the cord leaves a coating of black paint on the ground, and whenever his movement
1829 is clockwise, the cord leaves a coating of orange paint on the ground. The paint is dispensed
1830 regardless of whether there is already paint on the ground. The paints covers 1 gallon/unit², and
1831 Robert starts at $(1, 0)$. Each second, he moves in a straight line from the point $(\cos(\theta), \sin(\theta))$
1832 to the point $(\cos(\theta + a), \sin(\theta + a))$, where a changes after each movement. a starts out as 253°
1833 and decreases by 2° each step. If he takes 89 steps, then the difference, in gallons, between the
1834 amount of black paint used and orange paint used can be written as ...

1835

1836 **Training problem 4**

1837

1838

1839

1840

1841

1842 There are n players in a round-robin ping-pong tournament (i.e. every two persons will play
1843 exactly one game). After some matches have been played, it is known that the total number
1844 of matches that have been played among any $n - 2$ people is equal to 3^k (where k is a fixed
1845 integer). Find the sum of all possible values of n . The solution will be evaluated in a math
1846 environment.

1847

1848

1849 **Training problem 5**

1850

1851

1852

1853

1854 Let $\triangle ABC$ be a triangle with $AB = 4$ and $AC = \frac{7}{2}$. Let ω denote the A -excircle of $\triangle ABC$.
1855 Let ω touch lines AB, AC at the points D, E , respectively. Let Ω denote the circumcircle of

1836

$\triangle ADE$. Consider the line ℓ parallel to BC such that ℓ is tangent to ω at a point F and such that ℓ does not intersect Ω . Let ℓ intersect lines AB , AC at the points X , Y , respectively, with $XY = 18$ and $AX = 16$. Let the perpendicular bisector of XY meet the circumcircle of $\triangle AXY$ at P , Q , where the distance from P to F is smaller than the distance from Q to F . Let ray \overrightarrow{PF} meet Ω for the first time at the point Z . If $PZ^2 = \frac{m}{n}$ for relatively prime positive integers m , n , find $m + n$. The solution will be evaluated in a math environment.

1842

1843

1844

Training problem 6

1845

1846

1847

1848

1849

1850

1851

1852

1853

1854

1855

13 LHS Students attend the LHS Math Team tryouts. The students are numbered $1, 2, \dots, 13$. Their scores are s_1, s_2, \dots, s_{13} , respectively. There are 5 problems on the tryout, each of which is given a weight, labeled w_1, w_2, \dots, w_5 . Each score s_i is equal to the sum of the weights of all problems solved by student i . On the other hand, each weight w_j is assigned to be $\frac{1}{\sum s_i}$, where the sum is over all the scores of students who solved problem j . (If nobody solved a problem, the score doesn't matter). If the largest possible average score of the students can be expressed in the form $\frac{\sqrt{a}}{b}$, where a is square-free, find $a + b$. The solution will be evaluated in a math environment.

1853

Training problem 7

1854

1855

1856

1857

1858

1859

1860

Let $ABCDE$ be a pentagon with area 2017 such that four of its sides AB , BC , CD , and EA have integer length. Suppose that $\angle A = \angle B = \angle C = 90^\circ$, $AB = BC$, and $CD = EA$. The maximum possible perimeter of $ABCDE$ is $a + b\sqrt{c}$, where a , b , and c are integers and c is not divisible by the square of any prime. Find $a + b + c$. The solution will be evaluated in a math environment.

1861

1862

Training problem 8

1863

1864

1865

1866

1867

1868

1869

1870

1871

Let $\triangle ABC$ be a triangle with $AB = 4$ and $AC = \frac{7}{2}$. Let ω denote the A -excircle of $\triangle ABC$. Let ω touch lines AB , AC at the points D , E , respectively. Let Ω denote the circumcircle of $\triangle ADE$. Consider the line ℓ parallel to BC such that ℓ is tangent to ω at a point F and such that ℓ does not intersect Ω . Let ℓ intersect lines AB , AC at the points X , Y , respectively, with $XY = 18$ and $AX = 16$. Let the perpendicular bisector of XY meet the circumcircle of $\triangle AXY$ at P , Q , where the distance from P to F is smaller than the distance from Q to F . Let ray \overrightarrow{PF} meet Ω for the first time at the point Z . If $PZ^2 = \frac{m}{n}$ for relatively prime positive integers m , n , find $m + n$. The solution will be evaluated in a math environment.

1872

1873

Point P is in the interior of $\triangle ABC$. The side lengths of ABC are $AB = 7$, $BC = 8$, $CA = 9$. The three feet of perpendicular lines from P to sides BC , CA , AB are D , E , F respectively. Suppose the minimal value of $\frac{BC}{PD} + \frac{CA}{PE} + \frac{AB}{PF}$ can be written as $\frac{a}{b}\sqrt{c}$, where $\gcd(a, b) = 1$ and c is square-free, calculate abc . The solution will be evaluated in a math environment.

1878

1879

Training problem 10

1880

1881

1882

1883

1884

1885

1886

1887

1888

1889

Billy the baker makes a bunch of loaves of bread every day, and sells them in bundles of size 1, 2, or 3. On one particular day, there are 375 orders, 125 for each bundle type. As such, Billy goes ahead and makes just enough loaves of bread to meet all the orders. Whenever Billy makes loaves, some get burned, and are not sellable. For nonnegative i less than or equal to the total number of loaves, the probability that exactly i loaves are sellable to customers is inversely proportional to 2^i (otherwise, it's 0). Once he makes the loaves, he distributes out all of the sellable loaves of bread to some subset of these customers (each of whom will only accept their desired bundle of bread), without worrying about the order in which he gives them out. If the expected number of ways Billy can distribute the bread is of the form $\frac{a^b}{2^c - 1}$, find $a + b + c$. The solution will be evaluated in a math environment.

1890
1891

F.3 TTC FOR CODEELO

1892
1893
1894

In the following, we list the 10 most relevant problems selected by SIFT to improve performance on the CodeElo benchmark.

1895
1896
1897
1898
1899
1900
1901
1902
1903
1904
1905
1906
1907
1908
1909
1910**Training problem 1**

There are n monsters standing in a row. The i -th monster has a_i health points.

Every second, you can choose one alive monster and launch a chain lightning at it. The lightning deals k damage to it, and also spreads to the left (towards decreasing i) and to the right (towards increasing i) to alive monsters, dealing k damage to each. When the lightning reaches a dead monster or the beginning/end of the row, it stops. A monster is considered alive if its health points are strictly greater than 0.

For example, consider the following scenario: there are three monsters with health equal to $[5, 2, 7]$, and $k = 3$. You can kill them all in 4 seconds:

- launch a chain lightning at the 3-rd monster, then their health values are $[2, -1, 4]$;
- launch a chain lightning at the 1-st monster, then their health values are $[-1, -1, 4]$;
- launch a chain lightning at the 3-rd monster, then the ...

Training problem 2

Eshag has an array a consisting of n integers.

Eshag can perform the following operation any number of times: choose some subsequence of a and delete every element from it which is strictly larger than AVG , where AVG is the average of the numbers in the chosen subsequence.

For example, if $a = [1, 4, 3, 2, 4]$ and Eshag applies the operation to the subsequence containing a_1, a_2, a_4 and a_5 , then he will delete those of these 4 elements which are larger than $\frac{a_1+a_2+a_4+a_5}{4} = \frac{11}{4}$, so after the operation, the array a will become $a = [1, 3, 2]$.

Your task is to find the maximum number of elements Eshag can delete from the array a by applying the operation described above some number (maybe, zero) times.

A sequence b is a subsequence of an array c if b can be obtained from c by deletion of several (possibly, zero or all) elements. The solution will be evaluated in a code environment.

Training problem 3

There are n squares drawn from left to right on the floor. The i -th square has three integers p_i, a_i, b_i , written on it. The sequence p_1, p_2, \dots, p_n forms a permutation.

Each round you will start from the leftmost square 1 and jump to the right. If you are now on the i -th square, you can do one of the following two operations:

1. Jump to the $i + 1$ -th square and pay the cost a_i . If $i = n$, then you can end the round and pay the cost a_i .
2. Jump to the j -th square and pay the cost b_i , where j is the leftmost square that satisfies $j > i, p_j > p_i$. If there is no such j then you can end the round and pay the cost b_i .

There are q rounds in the game. To make the game more difficult, you need to maintain a square set S (initially it is empty). You must pass through these squares during the round (other squares can also be passed through). The square set S for ...

1944

1945

1946

1947

1948

1949

1950

1951

1952

1953

1954

1955

1956

1957

1958

1959

1960

Training problem 4

YouKn0wWho has an integer sequence a_1, a_2, \dots, a_n . Now he will split the sequence a into one or more consecutive subarrays so that each element of a belongs to exactly one subarray. Let k be the number of resulting subarrays, and h_1, h_2, \dots, h_k be the lengths of the longest increasing subsequences of corresponding subarrays.

For example, if we split $[2, 5, 3, 1, 4, 3, 2, 2, 5, 1]$ into $[2, 5, 3, 1, 4]$, $[3, 2, 2, 5]$, $[1]$, then $h = [3, 2, 1]$.

YouKn0wWho wonders if it is possible to split the sequence a in such a way that the bitwise XOR of h_1, h_2, \dots, h_k is equal to 0. You have to tell whether it is possible.

The longest increasing subsequence (LIS) of a sequence b_1, b_2, \dots, b_m is the longest sequence of valid indices i_1, i_2, \dots, i_k such that i_1, i_2, \dots, i_k and $b_{i_1}, b_{i_2}, \dots, b_{i_k}$. For ex ...

Training problem 5

Eve is a beginner stand-up comedian. Her first show gathered a grand total of two spectators: Alice and Bob.

Eve prepared $a_1 + a_2 + a_3 + a_4$ jokes to tell, grouped by their type:

type 1: both Alice and Bob like them;

type 2: Alice likes them, but Bob doesn't;

type 3: Bob likes them, but Alice doesn't;

type 4: neither Alice nor Bob likes them.

Initially, both spectators have their mood equal to 0. When a spectator hears a joke he/she likes, his/her mood increases by 1. When a spectator hears a joke he/she doesn't like, his/her mood decreases by 1. If the mood of a spectator becomes negative (strictly below zero), he/she leaves.

When someone leaves, Eve gets sad and ends the show. If no one leaves, and Eve is out of jokes, she also ends the show.

Thus, Eve wants to arrange her jokes in such a way that the show lasts as long as possible. Help her to calculate the maximum number of jokes she can tell before the show ends. The solution will be eval ...

Training problem 6

Solve the following coding problem using the programming language python:

zscoder has a deck of $n + m$ custom-made cards, which consists of n cards labelled from 1 to n and m jokers. Since zscoder is lonely, he wants to play a game with himself using those cards.

Initially, the deck is shuffled uniformly randomly and placed on the table. zscoder has a set S which is initially empty.

Every second, zscoder draws the top card from the deck. If the card has a number x written on it, zscoder removes the card and adds x to the set S . If the card drawn is a joker, zscoder places all the cards back into the deck and reshuffles (uniformly randomly) the $n + m$ cards to form a new deck (hence the new deck now contains all cards from 1 to n and the m jokers). Then, if S currently contains all the elements from 1 to n , the game ends. Shuffling the deck doesn't take time at all.

1998

1999

2000

2001

2002

2003

2004

2005

2006

2007

2008

2009

2010

2011

2012

2013

What is the expected number of seconds before the game ends? We can sho ...

Training problem 7

n pupils, who love to read books, study at school. It is known that each student has exactly one best friend, and each pupil is the best friend of exactly one other pupil. Each of the pupils has exactly one interesting book.

The pupils decided to share books with each other. Every day, all pupils give their own books to their best friends. Thus, every day each of the pupils has exactly one book.

Your task is to use the list of the best friends and determine the exchange of books among pupils after k days. For simplicity, all students are numbered from 1 to n in all tests. The solution will be evaluated in a code environment.

Training problem 8

You are given a rooted tree, consisting of n vertices. The vertices are numbered from 1 to n , the root is the vertex 1.

You can perform the following operation at most k times:

choose an edge (v, u) of the tree such that v is a parent of u ;

remove the edge (v, u) ;

add an edge $(1, u)$ (i. e. make u with its subtree a child of the root).

The height of a tree is the maximum depth of its vertices, and the depth of a vertex is the number of edges on the path from the root to it. For example, the depth of vertex 1 is 0, since it's the root, and the depth of all its children is 1.

What's the smallest height of the tree that can be achieved? The solution will be evaluated in a code environment.

Training problem 9

Back in time, the seven-year-old Nora used to play lots of games with her creation ROBO-Head-02, both to have fun and enhance his abilities.

One day, Noras adoptive father, Phoenix Wyle, brought Nora n boxes of toys. Before unpacking, Nora decided to make a fun game for ROBO.

She labelled all n boxes with n distinct integers a_1, a_2, \dots, a_n and asked ROBO to do the following action several (possibly zero) times:

Pick three distinct indices i, j and k , such that $a_i | a_j$ and $a_i | a_k$. In other words, a_i divides both a_j and a_k , that is $a_j \bmod a_i = 0, a_k \bmod a_i = 0$.

After choosing, Nora will give the k -th box to ROBO, and he will place it on top of the box pile at his side. Initially, the pile is empty.

After doing so, the box k becomes unavailable for any further actions. Being ...

Training problem 10

This is an interactive problem

You are given a grid $n \times n$, where n is odd. Rows are enumerated from 1 to n from up to down, columns are enumerated from 1 to n from left to right. Cell, standing on the intersection of row

2052 x and column y, is denoted by (x, y) .
 2053
 2054 Every cell contains 0 or 1. It is known that the top-left cell contains 1, and the bottom-right cell
 2055 contains 0.
 2056
 2057 We want to know numbers in all cells of the grid. To do so we can ask the following questions:
 2058
 2059 $x_1 y_1 x_2 y_2$, where $1 \leq x_1 \leq x_2 \leq n, 1 \leq y_1 \leq y_2 \leq n$, and $x_1 + y_1 + 2 \leq x_2 + y_2$. In other
 2060 words, we output two different cells $(x_1, y_1), (x_2, y_2)$ of the grid such that we can get from the
 2061 first to the second by moving only to the right and down, and they aren't adjacent.
 2062
 2063 As a response to such question you will be told if there exists a path between (x_1, y_1) and
 2064 (x_2, y_2) , going only to the right or down, numbers in cells of which form a palindrome.
 2065
 2066 For example, paths, shown in gr ...

2067
 2068
 2069
 2070
 2071
 2072
 2073
 2074
 2075
 2076
 2077
 2078
 2079
 2080
 2081
 2082
 2083
 2084
 2085
 2086
 2087
 2088
 2089
 2090
 2091
 2092
 2093
 2094
 2095
 2096
 2097
 2098
 2099
 2100
 2101
 2102
 2103
 2104
 2105